Joint Formation in the Caudal Fin Rays of *Danio rerio* (Zebrafish) During Fin Regeneration

Derek Sheppard

Master's Thesis

Thesis submitted to the faculty of graduate and postgraduate studies at the University of Ottawa.

In partial requirements for the degree of Masters of Science, Biology

Abstract

Danio rerio, more commonly called zebrafish, possess the ability to regenerate many of their organs and appendages including complete regeneration of the caudal fin back to its original size. The caudal fin consists of 16-18 fin rays (lepidotrichia) separated by interray tissue. These fin rays consist of bone segments that are partitioned by joints. Each bone segment consists of two oval shaped hemirays that form a tube-like structure that houses a multitude of tissues. During regeneration, the fin ray elongates through the distal addition of bone segments separated by newly formed joints. This is all regulated by a highly proliferative group of cells called the blastema located in the most distal portion of the regenerating fin ray. Our lab has been able to distinguish different stages of joint maturation during the regenerative process which has led to an interest in the effects of joint cell ablation during regeneration. A transgenic line of zebrafish that contained *lnta11* regulatory elements was found to give expression of a reporter in the joints of adult zebrafish. We used this regulatory element to drive expression of nitroreductase (NTR) in joint cells. In the presence of NTR, metronidazole (MTZ) induces ablation through initiation of the caspase dependent apoptosis cascade. Previous joint cell photoblation results in our lab indicated that joints may not be able to regenerate, we wanted to determine the results of complete ablation of joint cells during regeneration using the NTR/MTZ inducible targeted ablation technique. Surprisingly treatment with MTZ did not completely eliminate the joints during regeneration. However, there was a reduction in segment length and overall fin length of fish treated with MTZ compared to controls. Furthermore, as the concentration of MTZ is increased there is a proportional reduction in segment length of the fin regenerate. Although we failed to eliminate joints, the phenotype observed provided support for our proposed model of joint formation during regeneration. The creation of transgenic fish lines are underway to allow the separate ectopic

expression of two transcription factors; *sp7* (a known marker of osteoblast commitment) and *hoxa13a* (a hypothesized joint commitment factor) during regeneration.

Acknowledgments

I would first and foremost like to express my deepest gratitude to my supervisor Dr. Marie-Andrée Akimenko for her guidance and insight throughout my thesis, as well as providing me with a project I thoroughly enjoyed working on. I would like to thank the members of my thesis advisory committee Dr. Marc Ekker and Dr. Iain McKinnell for their guidance and providing constructive input throughout my thesis. I would like to give a special thanks to Jing Zhang who taught me a variety of techniques and equipment used throughout my masters. I would also like to thank members of the Akimenko lab: Robert Lalonde, Marissa Northorp, Eileen Hue-Phan, Hannah Nicholas, Samuel MacDonnell, Serina Khater, Andie Godo, and Qing ming for their input, encouragement, and entertainment throughout my masters. I would also like to thank members of the fish facility Bill Fletcher, Christine Archer, and Vishal Saxena.

Finally, I would like to thank my parents, Ken and Carol, for their continued support through my educational pursuits as well as the rest of my family. I would like to thank all my friends in Orangeville and all the friends I've made along the way.

Table of Contents

List of Figures

List of Abbreviations

2A	Self-cleaving peptide
4-OHT	4-hydroxytamoxifen, prodrug that allows translocation of Cre into nucleus when it is fused to ER
BMP	Bone morphogenetic protein, pathway involved in bone formation
Cre	Tyrosine recombinase enzyme from P1 bacteriophage. Cre recognizes and recombines loxp sites, allowing for DNA sequences located between loxp sites to be excised.
cx43	*connexin43*,
DAPI	4',6-diamidino-2-phenylindole, stains nucleus of cells
dpa	days post amputation
dpt	days post treatment
evx1	*Even-Skipped homeobox 1*, transcription factor
FGF	Fibroblast Growth Factor
GFP	Green Fluorescent Protein
Hoxa13a	Homeobox A13 orthologue A, transcription factor hypothesized to be involved in joint cell commitment
hpa	hours post amputation
hpf	hour post fertilization
Inta11	Mouse derived hoxa11 intron regulatory element. In this thesis, it indicates hoxa13a expression
MTZ	Metronidazole, drug that when reduced initiates cell apoptosis.
NTR	Nitroreductase, bacterial enzyme that reduces MTZ

PCNA	Proliferating cell nuclear antigen, labels cells that are undergoing proliferation
runx2a	Runt-related transcription factor 2 orthologue a
sp7	Osterix, transcription factor known to be involved in osteoblast commitment
Tg	denotes transgenic fish lines
TUNEL	Terminal deoxynucleotidyl transferase dUTP Nick End Labeling, used to label cells undergoing apoptosis
UV	Ultraviolet light
WT	Wild type
YFP	Yellow Fluorescent Protein

1 Introduction

1.1 Regeneration

The ability to regenerate tissues after injury varies widely among different species of animal. In higher vertebrates this ability has become limited (Maden, 1992), however, many aquatic species including aquatic urodelans, *Xenopus* (in juvenile stages), and teleost fishes have the ability to regenerate entire appendages once amputated (Akimenko, Marí-Beffa, Becerra, & Géraudie, 2003; Satoh, Mitogawa, & Makanae, 2015; Slack, Lin, & Chen, 2008). The goldfish was the first teleost fish to have its regenerative capabilities documented by Pierre Broussonet in 1789 when he noticed not only that injured fins regenerated, but that the caudal fin regenerated faster than all other fins (Pierre Marie Auguste Broussonet, 1789). Since that discovery teleost fishes have been used as model organisms, with zebrafish being one of the most popular models for caudal fin regeneration. Zebrafish fin regeneration is classified as epimorphic regeneration, because the cells dedifferentiate and begin to rapidly proliferate before differentiating once again reforming the lost appendage.

1.2 Zebrafish as a model organism for regeneration

There exist many model organisms which allow for the analysis and detailed studied of many scientific disciplines with the primary front runners including *Drosophila melanogaster, Saccharomyces cerevisiae,* and *Caenorhabditis elegans* to name a few. For the purpose of regeneration studies, *Danio rerio,* more commonly called the zebrafish has been extremely popular over the last few decades. Zebrafish produce large clutches of clear

embryos which undergo external development quickly, allowing for the study of vertebrate development from embryonic stages into adulthood in a relatively unhampered manner (Schier & Talbot, 2005). They can regenerate complex structures including structures of the central nervous system, heart, pancreas, liver, kidney, and complete regeneration of appendages (Bakkers, 2011; Chitnis, Dalle Nogare, & Matsuda, 2012; Y. Lee, 2005; Moss et al., 2009; Shin, Weidinger, Moon, & Stainier, 2012). The caudal fin has been the primary fin to study regeneration in zebrafish. It is the largest fin, it is bi-lobed, relatively simple cellular makeup, and regenerates quickly compared to other fins (Goldsmith, Iovine, O'Reilly-Pol, & Johnson, 2006).

1.3 Anatomy of the caudal fin

The caudal fin is the largest of the paired or unpaired fins of the zebrafish. It consists of 16-18 bony fin ray called lepidotrichia (Figure 1.3.1A), the majority of which bifurcate into two sister rays (Pfefferli & Jaźwińska, 2015). Each lepidotrichia consists of segments of bone, and each segment is made up of two hemirays which are oval shape bone deposits (Figure 1.3.1.C-D). The bone matrix is deposited by a group of cells known as osteoblasts (scleroblasts) which lie immediately under the epidermal cells and encase innervated and vascularized mesenchymal tissue (Borday et al., 2001; Gemberling, Bailey, Hyde, & Poss, 2013) (Figure 1.3.1C). The most distal 3-4 segments remain unmineralized and the most distal segment houses a cluster of unmineralized collagen fibers called actinotrichia that have been suggested to play a role in fin formation as well as fin regeneration (Borday et al., 2001; Durán, Marí-Beffa, Santamaría, Becerra, & Santos-Ruiz, 2011; Pfefferli & Jaźwińska, 2015). Each bone segment is separated from the next by joints termed fibrous joints which provide flexibility to the fin (Borday et al., 2001).

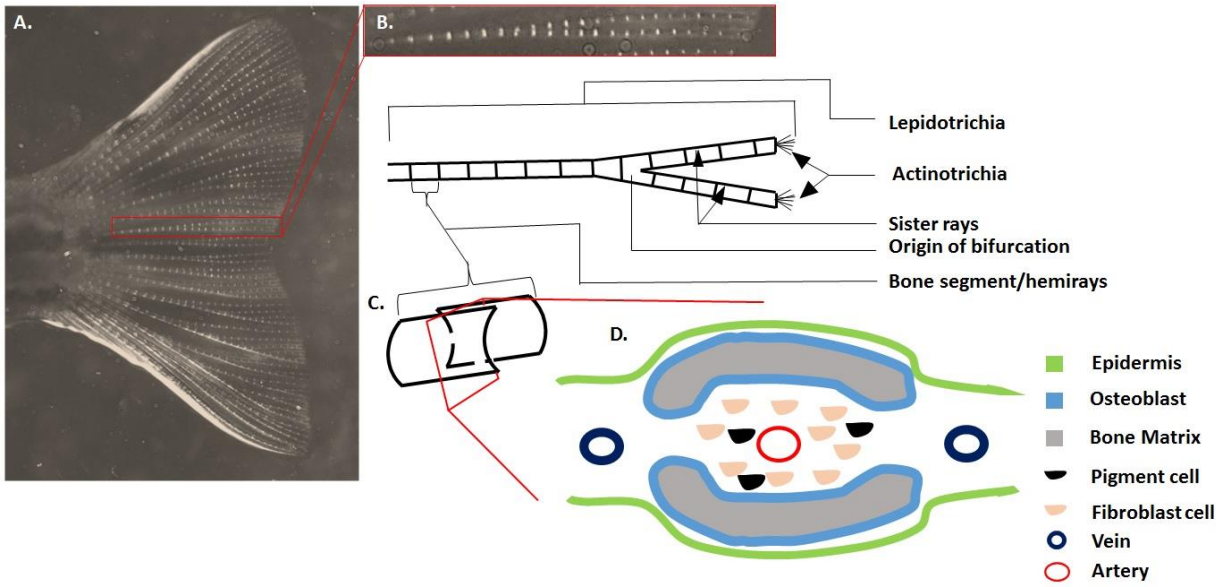

Figure 1.3.1 Anatomy of the zebrafish caudal fin

The zebrafish caudal fin (**A**) consists of 16-18 individual lepidotrichia (**B**). Each lepidotrichia consists of bone segments which are made of hemisegments that house a variety of cells types (**D**) and have actinotrichia at the distal most tip (**C**). Adapted from Akimenko et al., 2003; Tu & Johnson, 2011.

1.3.1 The bones

There are two different ways which bone can form; endochondral ossification and intramembranous ossification. In endochondral ossification mesenchymal cells differentiate into chondrocytes which form a cartilage template which resembles the future bone in both form and position (Hunziker, 1994; Mackie, Ahmed, Tatarczuch, Chen, & Mirams, 2008). After formation of the cartilage matrix the chondrocytes undergo hypertrophy and eventually die. The cartilage matrix created by the chondrocytes is then infiltrated by multiple cell types including osteoblasts which deposits bone on the cartilage (Mackie et al., 2008). This type of ossification is found in the endoskeleton of zebrafish caudal fins, the skeleton present at the base of the fin and that support the fin rays. Intramembranous ossification which forms the fins rays (exoskeleton of the fin rays) is much less studied (Abzhanov, Rodda, McMahon, & Tabin, 2007; Akimenko et al., 2003).

During intramembranous ossification mesenchyme condense and differentiate directly into osteoblasts. The osteoblasts then deposit the bone matrix directly, requiring no cartilage template (Abzhanov et al., 2007; Akimenko et al., 2003; Mackie, Tatarczuch, & Mirams, 2011).

1.3.2 The joints

There are multiple types of joints found in zebrafish that allow for the movement and flexibility of both the endo and exoskeleton. These joints are identical to or closely resemble joints found in mammals, making them good candidates for the study of joint formation and development (Askary et al., 2016; Hayes et al., 2013; Quarto & Longaker, 2006). Joints that connect flat bone to flat bones found in the skull are called sutures, this type of joint is found in the skulls of both mammals and fish (Kague et al., 2016; Quarto & Longaker, 2006). Sutures in the skull provides mechanical support for the bone plates while allowing for expansion of the brain during development and is also a site of osteogenesis (Kague et al., 2016; Laue et al., 2011; Quarto & Longaker, 2006). Zebrafish also have intervertebral discs that differ slightly from mammalian intervertebral disc in that they do not contain any fibrocartilage rings (*nucleus pulposus* and *annulus fibrosus*) between the vertebral bones, instead they have adipocytes (Askary et al., 2016). Similar to mammals, the adipocyte intervertebral discs are still susceptible to degeneration with aging, making them candidates to model osteoarthritis (Hayes et al., 2013). The most complex type of joint is the synovial joint, which connects bone with a fibrous joint capsule. Until very recently it was debated as to whether fish had joints similar to synovial joints found in mammals, and it turns out they are present in the jaw and endoskeleton of the pectoral fin (Askary et al., 2016). Zebrafish have many features of synovial joints that

are seen in mammals including articular cartilage, joint capsule, and synovium (Askary et al., 2016). Both jaw and pectoral joints of the zebrafish express homologues of *lubricin,* a marker of synovium in mammalian synovial joints (Askary et al., 2016; Rhee et al., 2005). All of the previously mentioned joints have been well studied in the zebrafish model, but the anatomy of the fibrous joint that connects bone segments in the fin rays of zebrafish remains relatively unknown. Mutant lines of zebrafish have been created that have altered joint patterning compared to wild type fish. In the *sof*^{b123} mutant the bone segments of the caudal fin are reduced in length as is the overall fin length, caused by a mutation in a protein believed to be involved in joint positioning (Iovine *et al.* 2005; Iovine & Johnson, 2000). In the *alf*^{dty86} mutant joint patterning is seemingly random and the caudal fin is longer compared to wild type fish due to a point mutation in a single gene (Haffter et al., 1996; van Eeden et al., 1996). Another zebrafish mutant is the *evx1*$^{-/-}$ null mutant that lacks a functional version of the transcription factor *evx1,* causing a lack of joints in fins (Schulte et al. 2011). In the context of fin regeneration the patterning and shape of the regenerating caudal fin has been sufficiently modeled mathematically, section 1.4 will expand on this area. (Rolland-Lagan et al. 2012). Despite all of this however, the cells that contribute to formation of the joint and its complete anatomy remain unknown.

1.4 Regeneration of the caudal fin

Upon injury to the caudal fin the process of regeneration will beginning almost immediately. This process occurs stepwise beginning with the contraction of epithelial tissue around the wound to seal it (Kawakami, 2010). This is followed by the formation of a wound epidermis. The wound epidermis is formed through the migration of the surrounding epithelial cells to create the wound epidermis, which is molecularly different

from the other epithelial tissues (Kenneth D. Poss et al., 2000). Once the wound epidermis is formed mesenchyme cells dedifferentiate and form the blastema, a cluster of proliferative cells. Once formed it is this group of cells that will begin to reform the injured appendage through cell differentiation creating the outgrowth (Akimenko et al., 2003; Kenneth D. Poss et al., 2000).

After amputation of the caudal fin and formation of the wound epidermis, the blastema will form at around the 24 hour mark (Kenneth D. Poss et al., 2000). This process begins with loosening and migration of mesenchymal cells as well as dedifferentiation of osteoblasts, leading to the formation of the blastema (Kenneth D. Poss et al., 2000; Singh, Holdway, & Poss, 2012). The blastema can be divided into two distinct regions; the proximal blastema and the distal blastema. The distal blastema is responsible for regulation of blastema cell proliferation through the Wnt/β-catenin signaling pathway, as well as indirectly monitoring osteoblast maturation through signals including fibroblast growth factor (Fgf) and bone morphogenetic protein (BMP) (Stewart, Gomez, Armstrong, Henner, & Stankunas, 2014; Wehner et al., 2014). The proximal portion of the blastema operates to ensure cells remain highly proliferative and is responsible for the redifferentiation of cells (Grotek, Wehner, & Weidinger, 2013; Münch, González-Rajal, & de la Pompa, 2013). The balance between these two processes is achieved through notch signaling, and when this signaling pathway is inhibited there is a decrease in blastema cell proliferation which leads to complete absence of a regenerate (Münch et al., 2013).

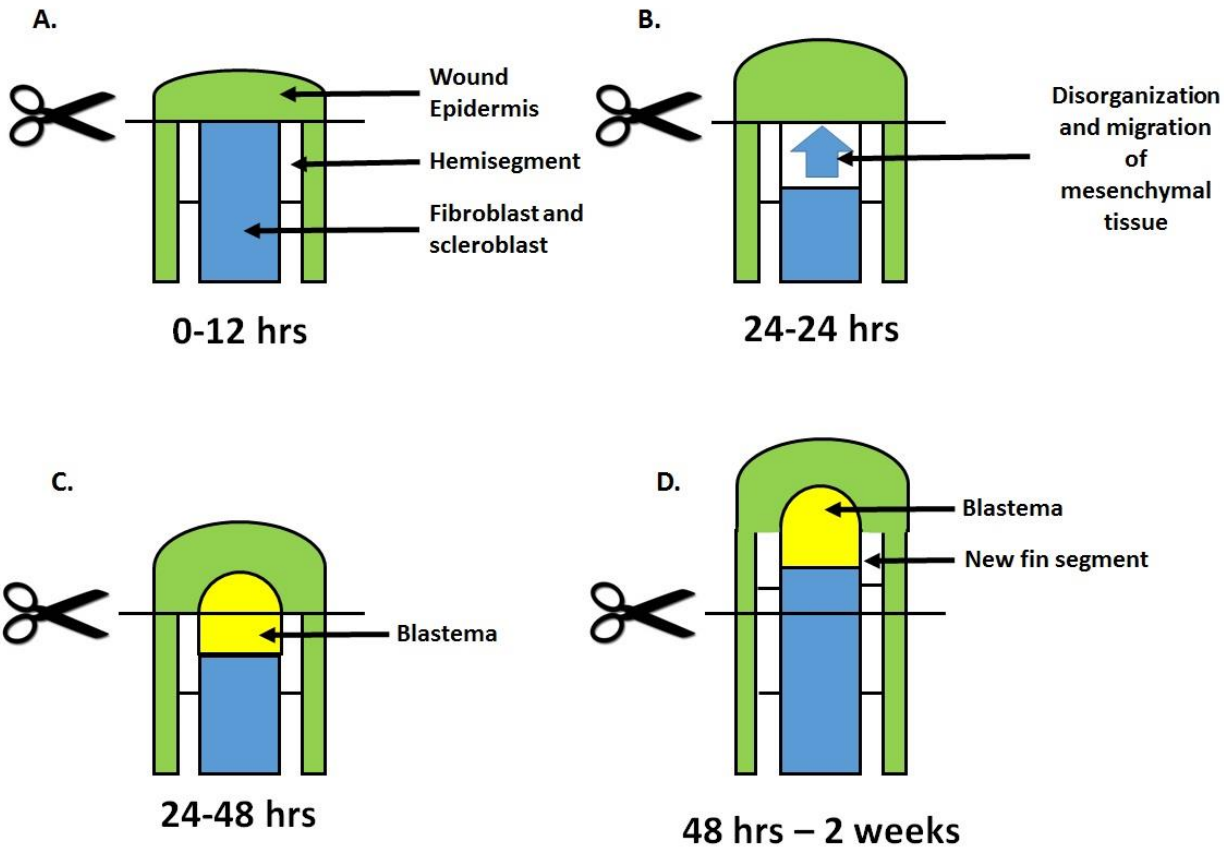

Figure 1.4.1 Stages of the regenerative process of leipidotrichia after amputation
After amputation, a wound epidermis is formed (**A**). This is followed by migration of mesenchyme cells (**B**) which eventually form the blastema (**C**). Once the blastema is formed outgrowth will occur until the appendage is restored to its original size and shape (**D**). Adapted from K D Poss et al., 2000.

1.4.1 Outgrowth

Once the blastema is formed, outgrowth will begin, adding bone segments to the distal portion of the regenerate until the appendage is restored to its original size and shape, though it will not be an exact replica. In order to reproduce the appendage two blastema mechanisms must act simultaneously; the distal blastema must remain undifferentiated and have a slow cycling rate while the cells of the proximal blastema must maintain high proliferation and differentiate into cells that form the new regenerate. The central portion of the proximal

blastema houses the highly proliferative mesenchyme cells and lateral to these are the dedifferentiated osteoblasts (Pfefferli & Jaźwińska, 2015).

1.5 Bone formation during regeneration

During the formation of the blastema, osteoblast cells of the stump dedifferentiate and migrate toward the wound (Knopf et al., 2011). These dedifferentiated cells downregulate expression of intermediate and late osteoblast markers but continue to express *runx2*, a pre-osteoblast marker (Knopf et al., 2011). These *runx2*$^{+}$ cells make up only a portion of the blastema, restricted to the lateral sides of the blastema under the epidermis (Knopf et al., 2011). The distal subpopulation of the *runx2*$^{+}$ cells maintain a highly proliferative state which has been suggested to be controlled by Wnt/β-catenin, and this is what provides the blastema with a continuous supply of *runx2*$^{+}$ cells during the course of regeneration (Stewart et al., 2014). As the *runx2*$^{+}$ cells move away from the distal source of Wnt they will upregulate *bmp2b,* activating the BMP signaling pathway (Stewart et al., 2014). BMP signaling is involved in the differentiation of the *runx2*$^{+}$ expressing pre-osteoblasts into osteoblasts through the upregulation the of the osteoblast commitment marker *sp7* and *dkk1b*, a Wnt pathway antagonist (Smith et al. 2006; Mao et al., 2001; Laforest et al., 1998). Following the expression of *sp7*is *osc* (osteocalcin, *bglap*), an osteoblast maturation marker used to label fully matured osteoblast (Gavaia et al., 2006). The presence of *runx2* does not only upregulate the expression of *sp*7, it also up regulates *collagen type 10A1* (*col10a1*), a short alpha-chain collagen that acts a marker for chondrocytes in mammals but is detected in both chondrocytes and osteoblasts of zebrafish (Eames, Amores, Yan, & Postlethwait, 2012; Komori, 2010). Studies have also suggested that *col10a1* plays a role in osteoblast formation (N. Li, Felber, Elks, Croucher, & Roehl,

2009; Smith et al., 2006). Lineage tracking of mature osteoblasts show that after amputation osteoblasts around the stump downregulate mature osteoblast markers and migrate toward the amputation plane and form part of the blastema (Knopf et al., 2011). During the outgrowth process these dedifferentiated osteoblasts will differentiate back into osteoblasts exclusively (Knopf et al., 2011). Although osteoblasts are fate restricted in regeneration, there is another source of cells which can produce osteoblasts if needed (Singh et al., 2012). In a study by Singh *et al*. osteoblasts were targeted for ablation using Tg(*sp7:NTR)* and treated with metronidazole to induce ablation (Singh et al., 2012). Prior to amputation osteoblasts were ablated and it was confirmed that osteoblasts were absent in the caudal fin (Singh et al., 2012). After amputation, fins regenerated in the same time course as controls and new bone was formed, indicating that there is another source of cells which can differentiate into osteoblasts (Singh et al., 2012). It has been suggested that bone and joint cells of the caudal fin are derived from a common lineage (Tu & Johnson, 2011). Using the conserved fugu *tryp1*>GFP lineage marker, over 100 zebrafish embryos were microinjected and those that had GFP expression in the caudal fin were investigated further (Tu & Johnson, 2011). Whenever there was expression of GFP in joint cells it was always accompanied by expression in osteoblast indicating they derived from a common lineage (Tu & Johnson, 2011). Our lab has recently found support for osteoblasts sharing a common lineage with joint cells. We examined expression of *runx2* expression and found that it overlapped with *sp7* expression but there was a small group of cells that created a protuberance that was *runx2*$^{+}$ but did not express the *sp7* osteoblast commitment marker (Figure 1.5.1). When this cluster of cells was ablated using laser photoablation technique, the corresponding joint was disrupted leading us to believe these were the newly forming joint cells.

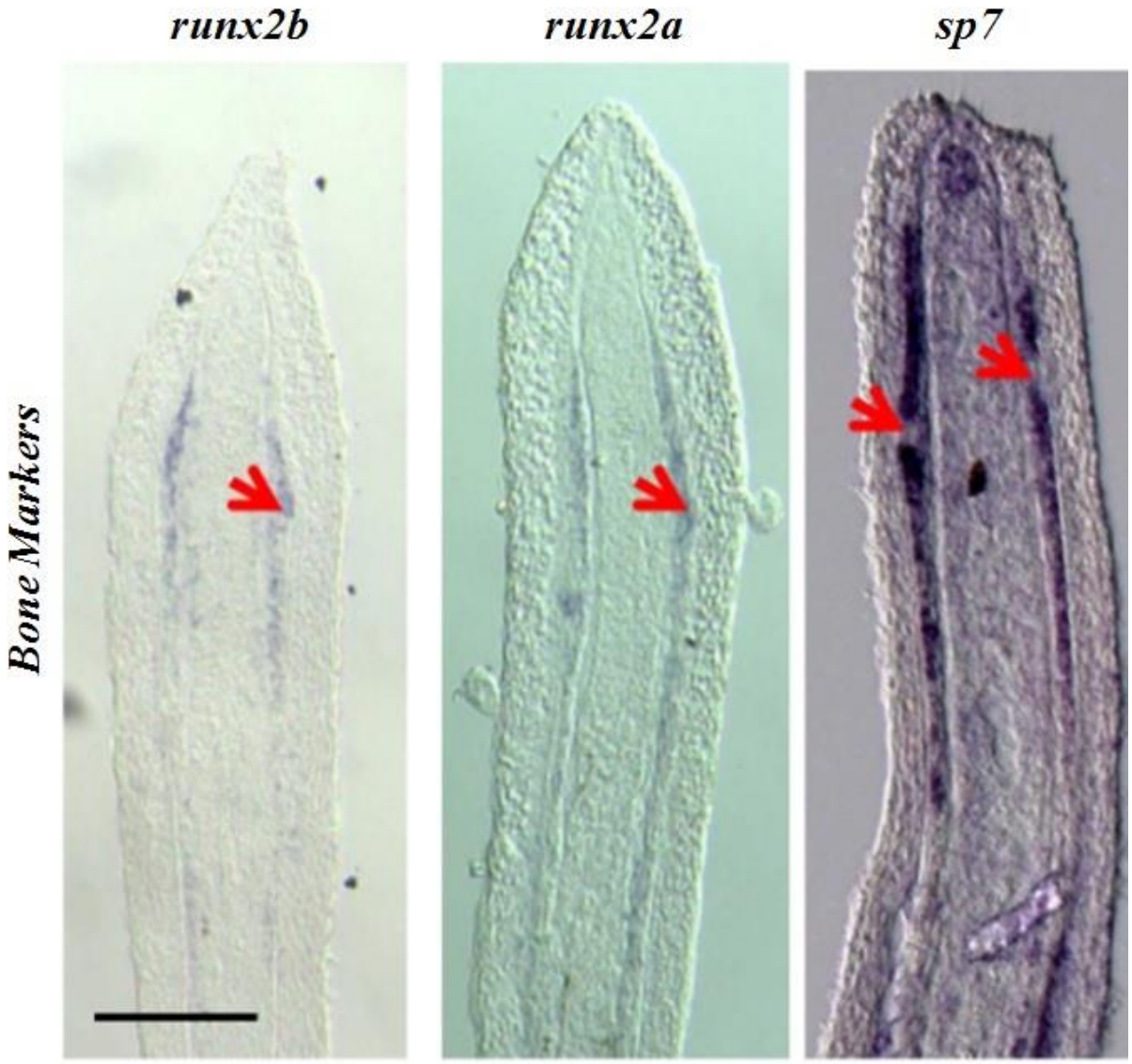

Figure 1.5.1 Overlap of expression *runx2a/b* and *sp7*
The expression of *runx2a* and *runx2b* share expression where joints are forming (red arrow) but in *sp7* expression there is expression that overlaps everywhere that *run2a/b* is except for where the joint is forming. McMillan unpublished.

1.5.1 Joint formation during regeneration

Joint formation during regeneration has not been as extensively studied as osteoblast regeneration in zebrafish. As previously stated the joint cells and osteoblasts share a common lineage, but how joint fate is derived is not fully understood. The first indication of joint formation is the condensing of cells in the presumptive joint region (distal part of regenerate)

into a single band of cells (Pacifici et al., 2006; Sims et al., 2009). This band then matures into two rows of joint cells that surround the newly forming joint (Pacifici et al., 2006; Sims et al., 2009). The transcription factor *evx1* of the family *even-skipped-related*-genes was discovered to have a pattern during regeneration that overlapped where joints appeared (Borday et al., 2001). The *evx1*$^{-/-}$ null mutant produces fin that lack joints during either development or regeneration, suggesting that *evx1* is required for joint formation (Schulte et al., 2011). In a gene expression analysis it was found that two other genes show expression in the joints in a pattern similar to *evx1* and they are *distal-less homeobox-5a* (*dlx5a*) and *matrix-metalloproteinase-9* (*mmp9*) (Yoshinari, Ishida, Kudo, & Kawakami, 2009). To determine the order in which these genes are expressed morpholino knockdowns were performed alongside comparison of expression in the *exv1*$^{-/-}$ mutant. In the *exv1*$^{-/-}$ mutant there is loss of *dlx5a* and *mmp9* expression, indicating they are both downstream of *evx1* (Ton & Iovine, 2013). In a morpholino knockdown of *dlx5a* in the regenerating fin there was a loss of *mmp9* expression, however a morpholino knockdown of *mmp9* did not result in loss of *dlx5a* expression and in both cases joint formation was disrupted indicating they do both play a role in joint patterning (Ton & Iovine, 2013). Investigations into connexin 43 (*cx43*), a component of connexons which form gap junctions between adjacent cells, has been shown to be negatively correlated to initiation of joint formation (Dardis et al., 2017; Ton & Iovine, 2013). The expression pattern of *cx43* in the regenerating joint is similar to that of *evx1* with a partial overlap (Iovine et al., 2005). During joint initiation the early joint marker *evx1* increases, and this increase correlates with a decrease in *cx43* (Dardis et al., 2017). Dardis *et al*. used transgenic a zebrafish line to increase in *cx43* expression in the cells surrounding the joints during regeneration by blocking *miR-133a*, which targets *cx43* for degradation (Dardis

et al., 2017). This upregulation of *cx43* led to a decrease in *evx1* expression as well as a significant increase in segment and regenerate length (Dardis et al., 2017). To supplement the transgenic finding the group treated WT fish with FK506, a calcineurin inhibitor that increases fin length. This resulted in a significant decrease in the expression of *evx1* in the treated fish and their fin rays failed to develop any joints during the treatment (Dardis et al., 2017). Finally when the group reduced *cx43* expression using an inducible transgenic zebrafish line that upregulated the *cx43* degrading target *miR-133a,* they found the result was premature expression of *evx1* in the regenerate that led to premature joint initiation and thus significantly shorter bone segments (Dardis et al., 2017). Other evidence that *cx43* is involved in the control of joint formation comes from the short fin (*sof*^{b123}) mutant. The phenotype observed in the *sof* ^{b123} zebrafish mutant, which manifests itself as reduced bone segment and fin length, is caused by mutations in *cx43* (Iovine et al., 2005). In the *sof* ^{b123} mutant the reduced *cx43* expression in the distal tip of the regenerate, which inhibits expression of *evx1,* allows for an earlier than normal initiation of *evx1* (Dardis et al., 2017). This earlier initiation of *evx1* means the expression will be seen more distal in the tip of the regenerating fin as the normal inhibition in that area is lifted (Dardis et al., 2017; Ton & Iovine, 2013).

The members of the joint forming pathway (*evx1*, *dlx5a*, *mmp9*) all had expression seen more distally than in controls indicating that joints were being formed earlier and causing the reduced segment lengths (Ton & Iovine, 2013). In another zebrafish mutant, *alf* ^{dty86}, which has an elongated fin and inconsistent bone segment length phenotype has been previously shown to have an increase in levels of *cx43* (Sims et al., 2009; van Eeden et al., 1996). In the *alf*^{dty86} there is a sporadic *evx1* expression that is believed to be caused by the

increased expression of *cx43* (Ton & Iovine, 2013). When morpholinos targeted to *cx43* were injected in fin regenerates of *alf*^{dty86} fish, there was a rescue of *evx1* expression, indicating that *cx43* does negatively regulate *evx1* expression and indirectly fin patterning in the regenerating fin (Ton & Iovine, 2013). Examining sections of the regenerating fin ray our lab has found a group of cells that cluster together creating a protuberance in the *runx2a/b*-expressing cells that were zns-5 positive, a marker of zebrafish osteoblast, indicating they were of osteoblast lineage (Figure 1.5.2A).

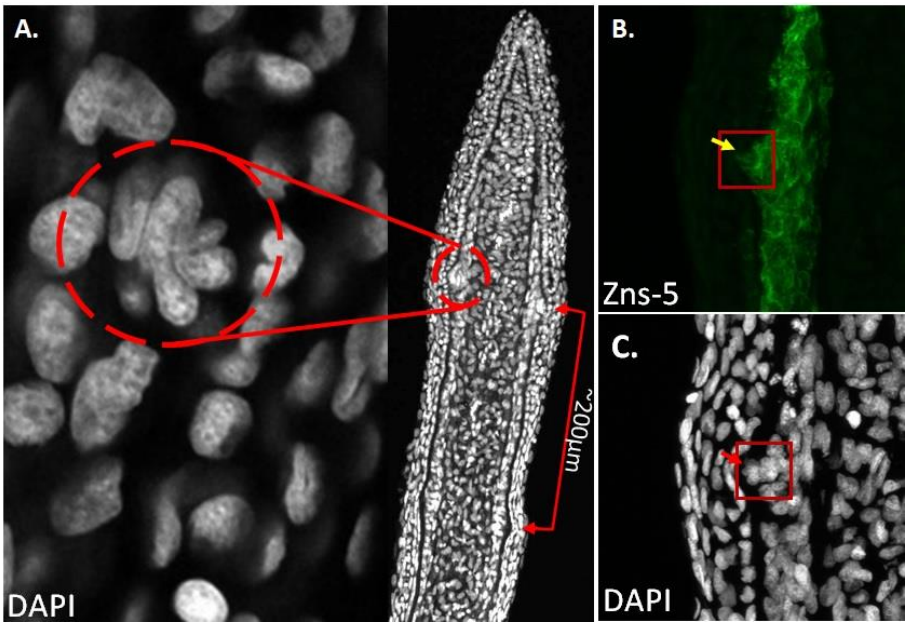

Figure 1.5.2 Cells that create protuberance appear to be pre-joint cells of osteoblast origin
Protuberance caused by clustering cells in the *runx2a* region are Zns-5 positive and spaced at appropriate distance for the next forming joint. Zhang unpublished.

This protuberance appears at a distance from the maturing joint cells where the next joint would begin to develop. Our lab examined the expression of osteoblast commitment marker *sp7* and mature marker *col10a1* and found that although there was an overlap of expression with *runx2a/b* this overlap did not include the protuberance created by the pre-joint cells.

(Figure 1.5.3). Known joint markers *evx1* and *pth1ha* along with hypothesized early joint marker *hoxa13a* were examined for expression in the pre-joint cells. In all three cases expression was observed in the area of the pre-joint cells and not overlapping the osteoblast cascade members (Figure 1.5.3). It was also noted at this point the *hoxa13a* expression had a gradient that peaked at the newly forming joint (Figure 1.6.2 and Figure 1.6.3). All of this together indicated that this cluster of cells that created the protuberance were early joint forming cells.

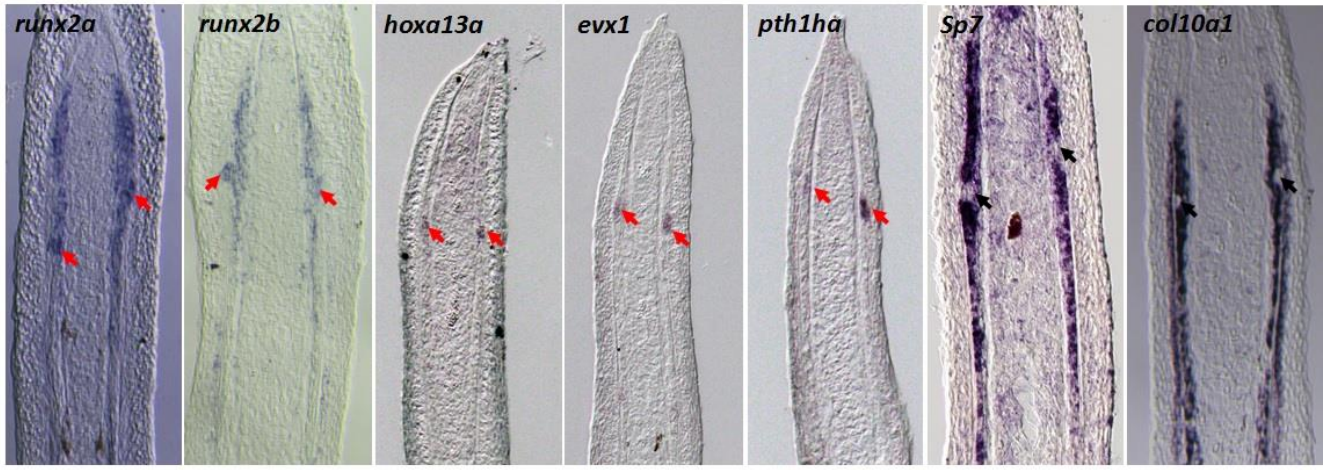

Figure 1.5.3 Osteoblast maturation cascade members are absent in cells that create the protuberance while joint maturation cascade members are present
Early osteoblasts markers *runx2a* and *runx2b* are expressed in cell protuberance (red arrows). Known (*evx1 and pth1ha*) and hypothesized (*hoxa13a*) members of the joint maturation cascade are present in the cells that create the protuberance (red arrows). Osteoblast commitment marker *sp7* and mature osteoblast marker *col10a1* are not expressed in the cell protuberance (black arrows). Zhang unpublished.

1.6 Hypothesized joint cell fate pathway

In an attempt to determine the sequential ordering of gene expression in newly forming joints, *evx1* expression was compared to both *hoxa13a* and *pth1ha* which both show

expression in cells of newly forming joints. Through comparison of the expression of the three markers in single and double *in situ* data, we were able to propose the sequential expression of these markers in the distal domain corresponding to the presumptive joint cells. When the expression of *hoxa13a* and *evx1* were compared *hoxa13a* expression was observed as the lone marker in presumptive region and there was never an instance where *evx1* was present in the absence of *hoxa13a*, suggesting the former is preceded by the latter. This pattern was also observed when expression of *evx1* and *pth1ha* were compared with only *evx1* ever appearing on its own. As would be expected when *hoxa13a* was compared to *pth1ha*, *hoxa13a* had lone expression in the presumptive joint cell region. Together this data suggests that expression of *hoxa13a* is upstream or in parallel of *evx1* which in turn precedes expression of *pth1ha* in early joint forming cells (Figure1.6.1).

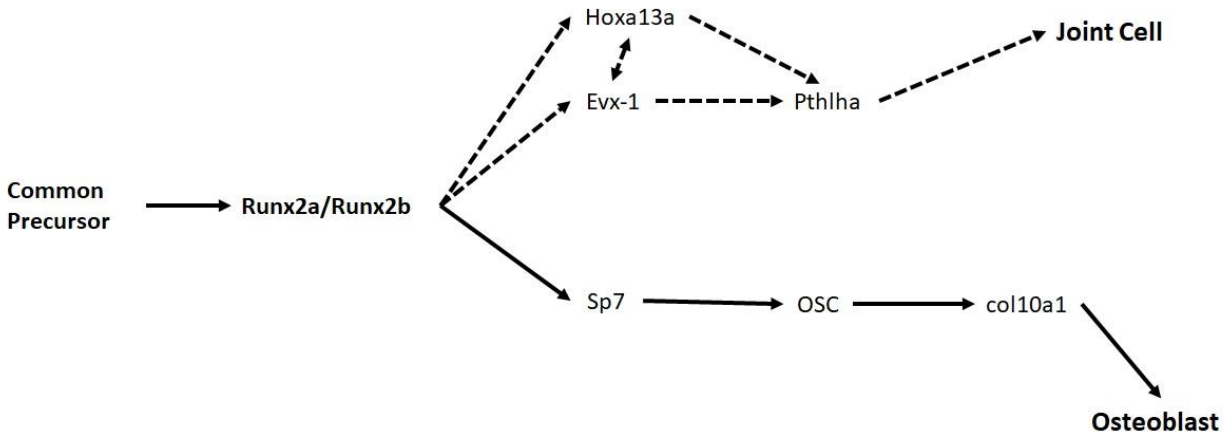

Figure 1.6.1 Hypothesized bipotency of runx2a^{+} cells.
A summary of the hypothesized joint cell forming pathway. It is known that when the runx2a^{+} cells express sp7 they will commit to becoming osteoblasts. It is hypothesized that when hoxa13a/evx1 are expressed in these cells that they will commit to becoming joint cells.

Support for this sequential order of early joint expression was provided when comparing the expression of *hoxa13a* and *pth1ha* in *evx1*$^{-/-}$ mutants, which lack fin ray joints,

to WT fish (Figure 1.6.22). In the *evx1*$^{-/-}$ mutants there was expression of *hoxa13a* in the region where a joint would be formed, and an absence of *pth1ha* (Figure 1.6.2E-F). In WT fish that have properly formed joints there is expression of both *hoxa13a* and *phtlha* where the joints are forming (Figure 1.6.2B-C).

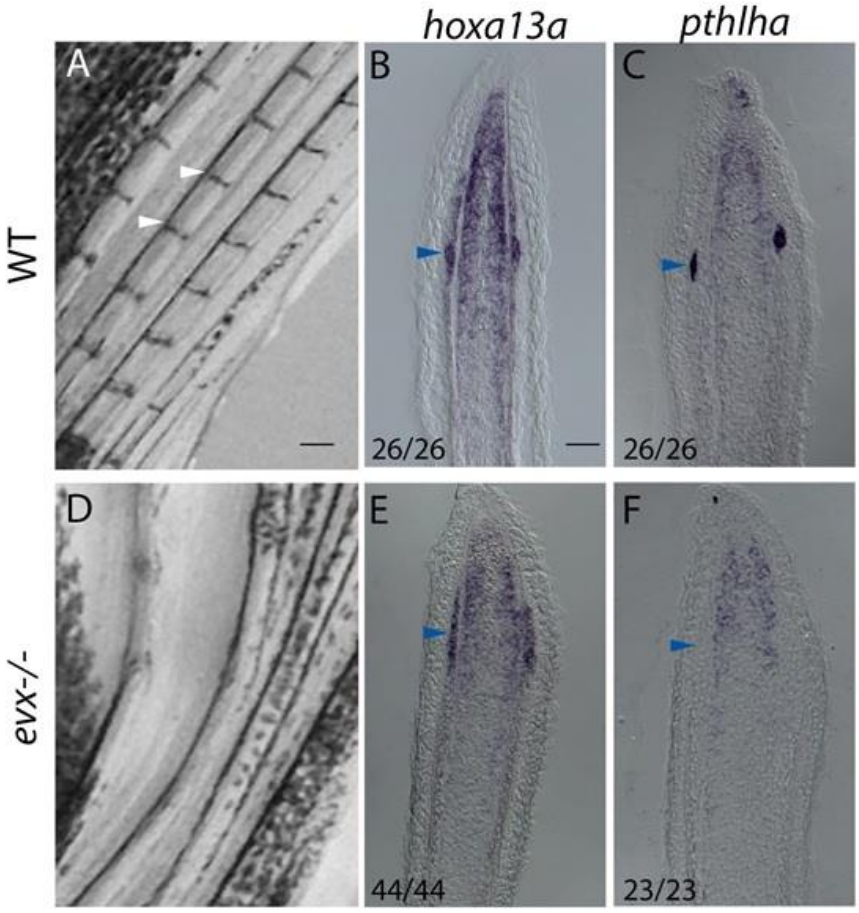

Figure 1.6.2 Expression of joint formation factors in *evx1*$^{-/-}$ mutant
In wild type fish with normal forming joints (**A**) the presence of *hoxa13a* in the area of presumptive joint cells in 26/26 sections (**B**) as well as the expression of *pthlha* in 26/26 sections(**C**). In the *evx1*$^{-/-}$ mutant which has no joints (**D**) there is an expression of *hoxa13a* in 44/44 sections (**E**). The presence of *pthlha* was not observed in the *evx1*$^{-/-}$ mutant in any of the 23 sections (**F**). section thickness was 18 µm.

1.6.1 Development of joint forming model

A member of our lab used laser photoablation, a technique used to ablate cells *in vivo*, to target the joint cells creating the protuberance during regeneration to determine if

they would regenerate. After ablation joint cells never regenerated which is not typical for zebrafish which have such incredible regenerative capabilities. This suggested that joint cells could only be formed at the initial joint cell commitment stage during regeneration and coupled with the proposed joint commitment pathway discovery allowed for the development of a joint formation model. The model is in part based off the discovered *hoxa13a* gradient of expression between the committed and presumptive joint cells (Figure 1.6.3). We propose that when a new joint is forming it leads to the synthesis of a joint inhibitor, and this inhibitor suppresses activation of *hoxa13a*. The expression of *hoxa13a* peaks in the presumptive joint cells and as the outgrowth continues to form, *hoxa13a* expression progressively increases as it moves further from the source of the inhibitor until it meets a threshold and the *runx2a/b* cells commit to becoming joints. Once these cells commit to becoming joint cells the process will repeat itself until regeneration is complete. We believe that joint cells can only form during this presumptive joint cell phase and if they are eliminated at this stage the regenerate will form without joints.

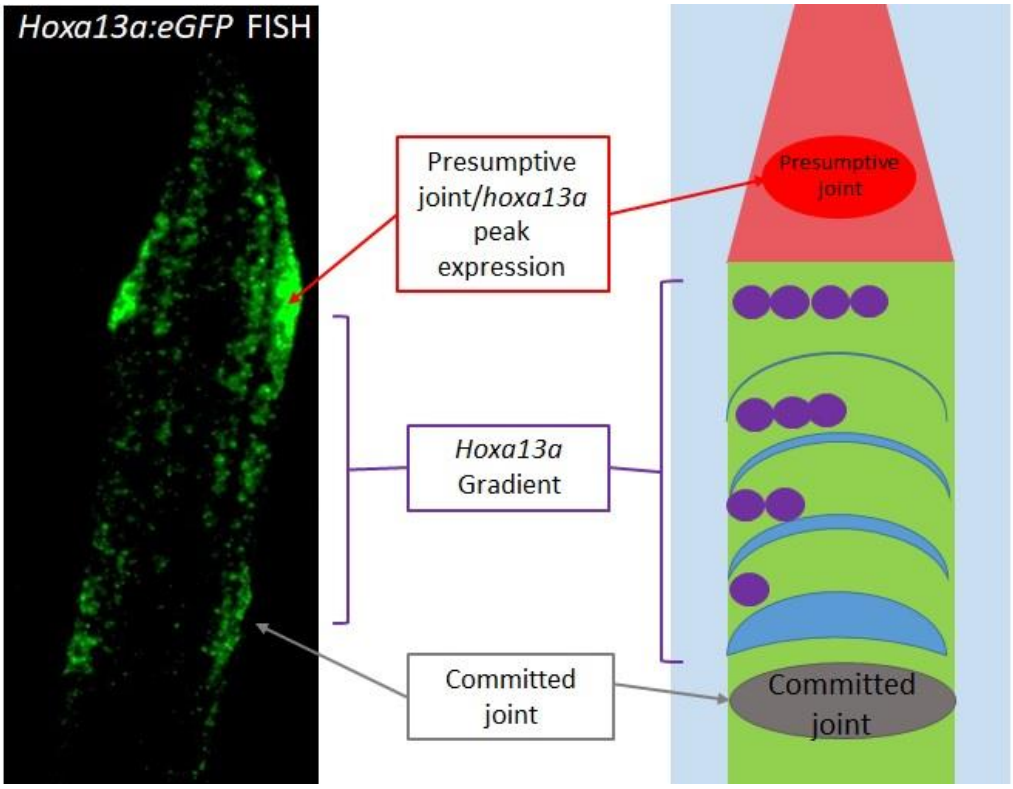

Figure 1.6.3 Joint forming model during regeneration
The observed *hoxa13a* gradient builds up as it gets further from the last forming joint which initiates a *hoxa13a* inhibitor (blue waves). As it gets further from the blastema, inhibitor strength weakens and *hoxa13a* hits a threshold in *runx2a*-expressing cells allowing for cells to commit to joints.

1.7 The Metronidazole/Nitroreductase system

The metronidazole/nitroreductase system, or more simply MTZ/NTR system, allows for inducible targeted cell ablation *in vivo*. Nitroreductase (NTR) is an enzyme of bacterial origin discovered in *E.coli* and in the presence of prodrugs including metronidazole (MTZ) targets cells for ablation (Knox, Friedlos, Jarman, & Roberts, 1988; Zenno, Koike, Tanokura, & Saigo, 1996). In the presence of NTR, MTZ is converted into a DNA cross-linking agent and this cross-linking leads to caspase initiated apoptosis in the targeted cells (Chen et al., 2011; Knox et al., 1988).

1.7.1 A method for the conditional genetic ablation of specific cell types in transgenic zebrafish

The metronidazole/nitroreductase (MTZ/NTR) genetic ablation method has been used extensively in transgenic zebrafish for targeted inducible ablation of a variety of cell types including pineal photoreceptors, pancreatic beta cells, cardiomyocytes, hepatocytes, macrophages, gonadal cells, skin cells, and retinal neuron subtypes (Ariga, Walker, & Mumm, 2010; Chen et al., 2011; Curado, Stainier, & Anderson, 2008; Gray et al., 2011; Hsu, Hou, Hong, Wu, & Her, 2010; X. Li et al., 2012; Pisharath, Rhee, Swanson, Leach, & Parsons, 2007). To target specific cells in zebrafish, transgenic zebrafish are created that express NTR under the control of a tissue-specific regulatory elements. When transgenic fish are placed in MTZ which can penetrate into tissue, it will induce apoptosis in the NTR-expressing cells with negligible bystander effects at 10mM concentrations and under (Summersgill, Schupp, & Raff, 1982; White & Mumm, 2013).

1.7.2 Targeted joint cell ablation in the regenerating caudal fin of zebrafish

In a separate, study our lab investigated the involvement of Hox genes and their role in the fin-to-limb transition, specifically looking at *Hoxa11* (Kherdjemil et al., 2016). In this study, a mouse-specific regulatory element named *Inta11* was identified. This element was shown to be controlled by *Hoxa13* and *Hoxd13* based on ChIP analysis. When the function of this enhancer was analyzed in transgenic zebrafish it was able to activate GFP reporter expression in the embryonic fins in a domain overlapping with *hoxa13a* domain of expression. Interestingly, in adult transgenic fish that used the *Inta11*regulatory elements to drive GFP reporter expression a pattern similar to that of *hoxa13a* was observed including in the joint at all differentiation stages.

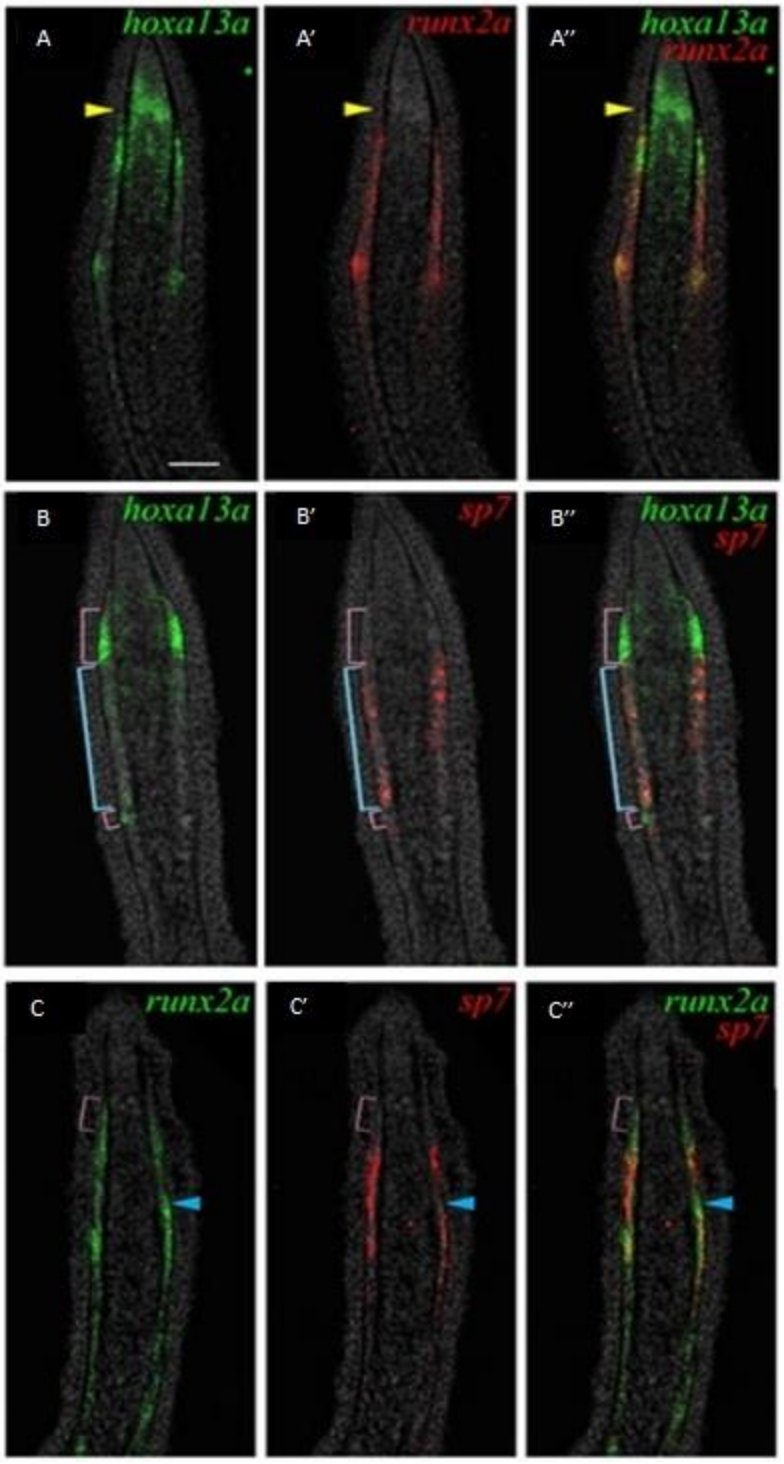

Figure 1.7.1 Expression of hoxa13a and sp7 are largely independent of one another during regeneration

The expression pattern of *hoxa13a* overlaps with *runx2a* expression and is in the area of the presumptive joints (yellow arrow) (**A**). The expression of *sp7* and *hoxa13a* only slightly overlap in osteoblasts, and *sp7* isn't found in the joint forming/committed regions (**B**). *sp7*

expression does overlap with *runx2a* but is not expressed in joint forming regions (**C**).

In our lab the transgenic zebrafish line Tg(*inta11-β-globin:YFP-2A-NTR*) was created to target all stages of joint cells for ablation. This transgenic line uses the *Inta11* regulatory elements along with the β-globin minimal promoter to drive expression of yellow fluorescing protein (YFP), a 2A self-cleaving peptide, and nitroreductase (NTR). In the joint cell of these transgenic fish the YFP:2A:NTR sequence will be transcribed as one long piece of mRNA, but during translation the 2A peptide is 'skipped' by the ribosome and undergoes proteolytic cleavage leaving equimolar concentrations of the proteins upstream and downstream of it (Ryan, King, & Thomas, 1991). In the absence of metronidazole (MTZ) the joint cells will express YFP, appearing yellow under UV, and NTR which is harmless on its own (Curado et al., 2007). In the presence of NTR, MTZ is converted to the DNA cross-linking agent, initiating the apoptotic cascade eliminating the joint cells (Figure 1.7.2).

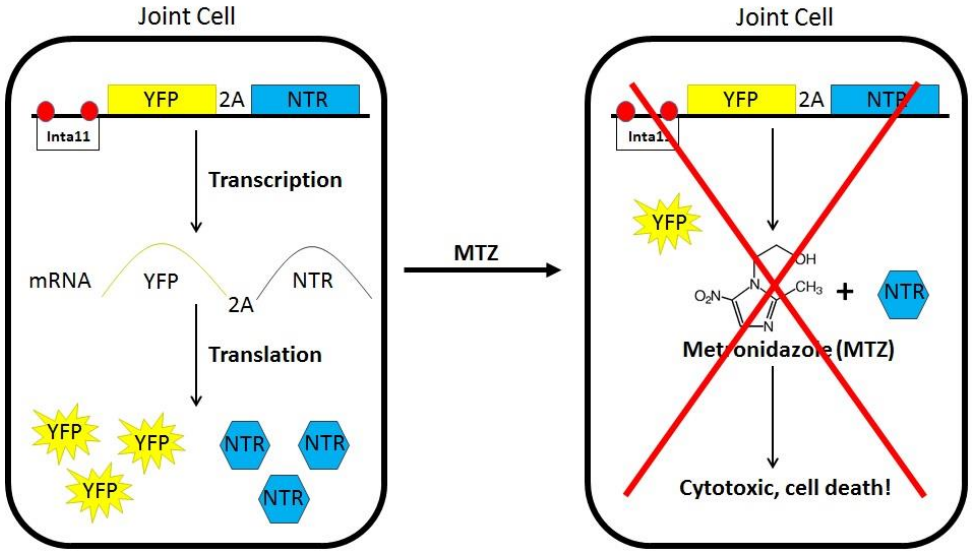

Figure 1.7.2 How metronidazole treatment leads to ablation of joint cells
In the absence of MTZ the joint cells will synthesize YFP and NTR in equimolar concentrations which is harmless to the cell. In the presence of NTR, MTZ will be reduced and lead to initiation of the caspase-dependent apoptotic cascade.

1.8 The Cre/loxP Recombinase system

The Cre/loxP system allows for mediated site-specific DNA recombination, first discovered in bacteriophage (Sternberg, 1981). The loxP site consists of 13 bp inverted repeats separated by 8 bp asymmetric spacer region, the Cre recombinase is a 343-amino acid monomeric protein. DNA sequences that are flanked by loxP will be excised by the Cre protein (Hoess, Wierzbicki, & Abremski, 1986). This system allows for inducible expression of genes by controlling Cre expression with an inducible promoter and has been modified for use in zebrafish (Thummel et al., 2005). More recently Cre has been fused to a mutant estrogen receptor creating Cre^{ERt2}, which on its own will not be able to excise DNA as it will remain in the cytoplasm (Hans, Kaslin, Freudenreich, & Brand, 2009). In the presence of the drug tamoxifen, which binds to the mutated estrogen, Cre^{ERt2} translocates to the nucleus where Cre will recognize the loxP sites and excise the DNA sequences flanked by them (Hans et al., 2009).

1.9 Objectives of the study

In this thesis, the regenerative capability of joint cells of the caudal fin of zebrafish is studied to determine if joint forming cells and osteoblast share a common lineage. We wanted to examine the effects of ablation of joint cells in the fin ray regenerate on the joints and bones, and to determine if the joint cells can regenerate following ablation. We also wanted to determine the role of *hoxa13a* in joint formation and maintenance. Lastly, we wanted to determine if ectopic expression of *sp7* is able to override joint cell commitment in the common lineage cells. By eliminating these cells throughout the course of regeneration we attempt to confirm if they have the ability to regenerate. There are three objectives that will test this:

1) Ablation of joint cells using MTZ/NTR: Using the *Inta11* regulatory elements, NTR expression will be driven in the presumptive and maturing/mature joint cells. They will be targeted for ablation with MTZ and the regenerate will be monitored for joint formation.

2) Ectopic expression of *sp7* in presumptive joint cells during regeneration: The transcription factor *sp7* is the osteoblast commitment marker in the pre-osteoblast *runx2a*-expressing cells. Since the *runx2a*-expressing cells are the common lineage between joint and osteoblasts, by expressing *sp7* in all *runx2a*-expressing cells including the presumptive joint cells we expect to control their fate and see a fin regenerate form without joints.

3) Ectopic expression of *hoxa13a* in *runx2a* expressing cells during regeneration: The presumptive joint cells in the *runx2a* region show an early expression of *hoxa13a* indicating it may play a role in joint cell commitment. By expressing *hoxa13a* in all *runx2a* cells during regeneration we hope to force the fate of all *runx2a* cells to become joints, creating a regenerate that is free of osteoblasts.

2 Materials and Methods

2.1 Zebrafish maintenance

2.1.1 Zebrafish care

Zebrafish were housed in the University of Ottawa Fish Facility. Zebrafish were kept at a constant temperature of 28.5˚C with a 14 hours light from 9am until 11pm followed by darkness from 11pm until 9am as is standard conditions (Westerfield, 2007). Zebrafish care and experimentation strictly followed the Canadian Council on Animal Care (CCAC) guidelines.

2.1.2 Zebrafish husbandry

Breeding for stock replenishment or microinjection followed a protocol similar to the false bottom traps outlined by Westerfield (2007). The main divergence from the outlined protocol was filter collection of embryos using a sterilized mesh strainer instead of a siphon. Two females and a single male were placed in false bottom traps and separated by a clear plastic divider. In the four days leading up to breeding, feeding of the fish was increased to twice a day; once in the morning and once in the afternoon.

For stock replenishment purposes embryos were collected and stored in E3 embryo media (5mM NaCl, 0.17mM KCl, 0.33mM CaCl2, 0.33mM MgSO4, 6-12 µM methylene blue). Between 12-30 hpf embryos underwent a sterilization process that began with a 10-minute bleach bath in 0.003% NaOCl solution, followed by a neutralization bath for 1 minute in 0.05% Na2S2O3 solution (Sigma-Aldrich), and finally two 2 minute rinse cycles in E3 embryo medium. At 5 – 7 dpf larvae were moved to a juvenile growth facility where their diet and growth was strictly monitored by the fish facility staff until sexual maturity was reached.

Breeding for microinjection followed the same protocol as stock replenishment with the only notable exception being that embryos were collected after 15 minutes of breeding to ensure that they would still be in the 1-2 cell stage which is the standard for injecting (Westerfield, 2007).

2.2 Fin amputation

Zebrafish were anesthetized using 0.24 mg/ml of tricaine (a general anesthetic commonly used for fish research) in UV sterilized water (Canadian Council on Animal Care, 2005). Anesthetized fished were placed onto a dry petri dish and their caudal fanned out to

what was considered to be a natural posture to ensure a straight cut. Cuts took place under a dissection microscope using a scalpel blade. The fins were cut perpendicular to the fin rays two segments below the most proximal bifurcation. After amputation fish were placed in a recovery tank containing UV sterilized water.

2.3 Metronidazole treatments

After standard amputation of the caudal fin of adult zebrafish, the fish were treated in 5, 10, or 15 mM metronidazole (MTZ) dissolved in UV treated water containing 1% dimethyl sulfoxide (DMSO), which is added to aid in the solubilization and enhanced penetration of MTZ (Curado et al., 2008). This initial treatment began at 2.5 dpa and was run for 30 hours with the fish kept in darkness as MTZ degrades in light. After the 30 hours in 10 mM fish were moved to 2.5 mM MTZ solution where they remained in darkness until 7 dpa.

2.4 Cryo-sectioning of fins

Fins were fixed overnight at 4˚C in 4% PFA then washed twice for 5 minutes in PBS (137 mM NaCl, 2.7 mM KCl, 4.3 mM Na2HPO4, 1.47 mM KH2PO4, adjusted to a final pH of 7.4). The fins then underwent dehydration starting with two 5-minute washes in 100% methanol at room temperature and stored at -20˚C. Once ready to be used fins were rehydrated in a series PBS washes. The fins were placed into 24-well dish and embedded by pouring 1.5% agar and 5% sucrose in 1X PBS that had been heated over the fin. The fin was then adjusted in molten agar solution and left to solidify. Once solid, the agar blocks containing the fins were trimmed to desired size and left overnight in 30% sucrose in 1X PBS solution at 4˚C. The agar blocks were covered in OCT before use and underwent a

freezing protocol. Sections were cut 18 µm thick were transferred to Superfrost/Plus slides, they were left at RT for 30 minutes before being placed at -20˚C.

2.5 TUNEL assays on sections

Sections were allowed to defrost at room temperature for a minimum of one hour, or overnight at 4˚C. Once the required temperature was reached slides underwent a permeabilization step beginning with a 15-minute rinse in 0.3% Triton-X 100 in PBS and adjusted to a pH of 7.4. The permeabilization step was followed by two 5-minute washes in PBS. The slides were then incubated in a proteinase K (PK) solution (5 ug/ml PK, 1M Tris HCl pH 8.0, 0.5M EDTA, dH_2O) for 15 minutes followed by two more 5-minute rinses in PBS. The sections were then fixed for 20 minutes in 4% PFA in PBS followed by two more 5-minute rinses in PBS. A positive control slide was prepared at this time point. The control slide was allowed to dry before being covered in a DNase I solution (DNase I, DNase I buffer, H_2O) for 10 minutes. After the DNase I incubation the slide was rinsed twice for 5 minutes in PBS. The TUNEL reaction mix from the *In Situ* Cell Death Kit (Roche) was applied to the slides once dried and covered with a cover slip before being placed in the dark for one hour at 37˚C. Once the incubation was complete the slides were rinsed in PBS containing 1:10000 DAPI for 5 minutes followed by two washes for 5 minutes in PBS. Slides were once again allowed to dry and mounted using Aqua-Mount mounting medium (polyscience) and left to dry overnight in the dark before being viewed. Pictures were taken using a Zeiss LSM 510/AxioVert 200 confocal and zen2009 software

2.6 PCNA assays on sections

Sections were allowed to defrost at room temperature for a minimum of one hour, or overnight at 4˚C. After room temperature was reached the antigen retrieval step began

starting with a 20-minute bath at 98˚C in 10 mM sodium citrate and 0.05% tween-20 corrected to a pH of 6.0. Sections were allowed to cool to room temperature for 15 minutes before being rinsed three times in PBS for 5 minutes. The section was then bathed in blocking solution (0.2% Triton X-100 and 2% Calf Serum in PBS) at RT for 2 hours. After blocking was complete the sections were incubated in solution containing the primary antibody anti-PCNA (Dako) at 1:250 in blocking solution. 200µl of the solution was added to cover the slide and the sections were incubated overnight at 4˚C in a humidifying chamber. Sections were then rinsed in four 10 minutes bathes in PBS-tween 20 (PBST). The secondary antibody, Alexa Fluor® 488 goat, anti-mouse IgG (Life Technologies) was diluted in PBST to 1:500 and 200µl of the solution was used to cover the slide and once again it was left to incubate for 3 hours at room temperature in a humidifying chamber. The sections were counter stained in 1:10000 DAPI in PBST for 10 minutes followed by three 10 minutes rinses in PBST and finally a 5-minute water rinse to remove salts. Slides were allowed to dry and mounted using Aqua-Mount mounting medium (polyscience) and left to dry overnight in the dark before being viewed. Pictures were taken using a Zeiss LSM 510/AxioVert 200 confocal and zen2009 software

2.7 Statistical analysis

All measurement data were collected using ImageJ version 1.48 and using a known scale bar to set a proper measure to get all measurements in mm. All measurements were performed twice and averaged in an effort to eliminate human error. Bone segment length was measured from the center point of the proximal joint to the center point in the distal joint.

Statistical data was generated using GraphPad Prism version 7.03. To determine statistical relevance, the Mann-Whitney test was used. Groups were compared directly to one another to determine significant differences. A non-parametric test was chosen because the data did not meet the criteria to use a parametric test and the data collected would be better represented by the median.

In Figure 3.2.4 the Mann-Whitney test showed there was no statistical difference between the Tg(*NTR*) treated with DMSO and WT treated with MTZ and so in subsequent comparisons were omitted.

2.8 Assessing Joint Quality

Joints were assessed on the quality of the white line that bisected the fin rays when observed using a bright field microscope. This white line is light coming through the actual joint, and if it is a distinct white line then the joint formed as it does in wild type fish. Currently this is the best option to assess joint quality since many of the components that comprise the fibrous joints in the caudal fin still need to be determined. It should be noted that if the joints between hemirays do not perfectly align, two white lines may be observed, this does not mean that the joint is of poor quality. A poor quality joint will have a weaker white line as the distinct joint gap did not form properly and less light gets through. The line may also be curved or angled instead of perpendicular to the fin ray.

3 Results

This section will begin with a qualitative assessment of the results of the MTZ/NTR experiments focusing on joints during regeneration. This will be followed by the quantitative assessment of the results of the MTZ/NTR experiment.

3.1 Mouse derived *Inta11* drives reporter expression in joint cells

The transgenic fish line previously created by a member of our lab and described above drives expression of YFP in the joint cells, actinotrichia-forming cells, and cells of the blastema in adult zebrafish throughout the course of regeneration (Figure 3.1.1 A-D). This expression pattern in the joints can be seen both distal and proximal to the plane of amputation, but consistently appeared brighter distally with peak expression in the area of the blastema. Prior to bifurcation of the fin rays the expression of YFP appeared to elongate in the proximal-distal direction and once bifurcation is complete expression is once again confined to joints, actinotrichia-forming cells and blastema.

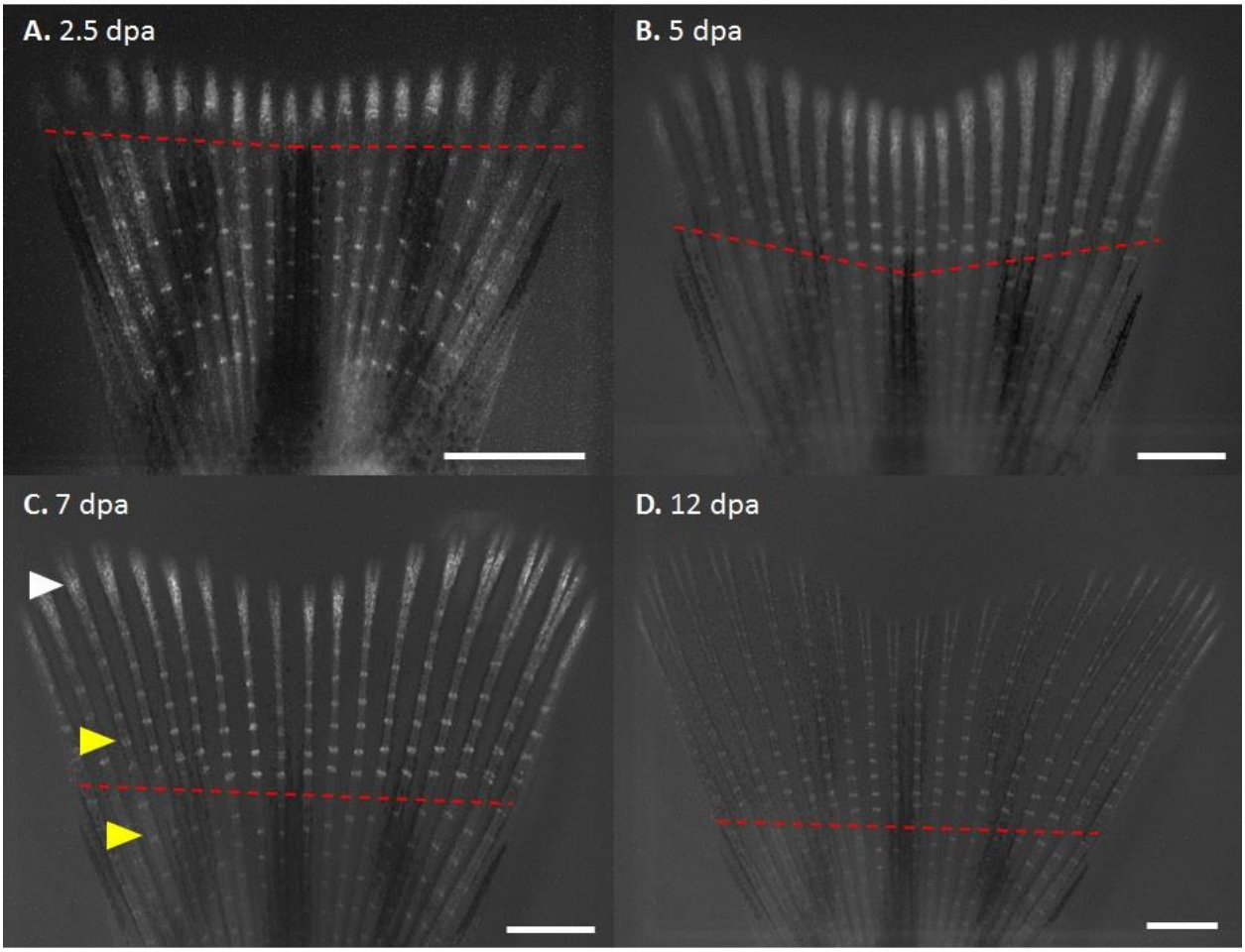

Figure 3.1.1 Transgenic line using *Inta11* regulatory elements gives YFP reporter expression in joints at all stages
*Inta11*drives expression of YFP in the joints (yellow arrow) and distal portion of the fin ray regenerate (white arrow) shown here from 2.5 days post amputation (dpa) until 12 dpa. Joint proximal and distal to the plane of amputation (red dashed line) express YFP. All scale bars are 1mm.

3.2 Elimination of joint cells during regeneration using metronidazole

To determine if the cells expressing *hoxa13a* during regeneration do have a role in the joint cell formation, we opted to ablate joint cells including the early forming joint cells during regeneration using the *Inta11* regulatory elements and β-globin minimal promoter (the latter of which is activated by *hoxa13a*) to express nitroreductase (NTR). If the cells expressing *hoxa13a* were eliminated in the presence of MTZ and joints failed to form, this

would provide support that cells expressing *hoxa13a* have an early role in joint cell formation during regeneration.

Before the MTZ trial to eliminate joints began, concentrations of 5, 10, 15, and 20 mM MTZ were used to determine the MTZ toxicity on adult (older than 3 months) wild type (denoted as WT in subsequent text) fish after 24, 30, and 48 hours of treatment. Fish were grouped into three categories; experimental - treated with MTZ and 1% dimethyl sulfoxide (denoted as DMSO in subsequent text), 1% DMSO control, and H_2O control. The experimental group was further divided into the 5, 10, 15, and 20 mM concentration groups. Each group contained three fish that were monitored over the aforementioned time course. The fish in 20 mM MTZ group died before the 24-hour mark was reached. The 15 mM MTZ treated fish were exhibited symptoms at 24 hours that suggested adverse effects brought on by the MTZ which included upside down swimming, reduced frequency and erratic breathing as well as a general inability to maintain upright. Fish in both 5 and 10 mM MTZ treated groups appeared to be unaffected by the MTZ throughout the time courses. 10 mM was chosen as the concentration to use as the adult fish appeared to be healthy after the trial and success has been observed at this concentration and lower in eliminating cells in adult and larvae zebrafish (Cox, Zhang, Pope, & Voigt, 2016; Petrie, Strand, Yang, Rabinowitz, & Moon, 2015).

To examine if these conditions were sufficient to eliminate joints during regeneration *Tg(Inta11-β-globin:YFP-2A-NTR)* fish, a line readily available, was used as the *Inta11* regulatory elements gave expression in the joint forming cells during regeneration in adults. The experiment used five groups of three fish; two *Tg(Inta11-β-globin:YFP-2A-NTR)* groups (denoted as *Tg(NTR)* in subsequent text) one treated with 10 mM MTZ and the other

with 1% DMSO, and three WT groups; 10 mM MTZ, DMSO, and H_2O. It was our belief that if the *Tg(NTR)* DMSO control formed a regenerated fin that mirrored both the WT DMSO and WT H_2O control then the *Tg(NTR)* H_2O control group could be omitted in the interest of limiting the amount of fish that would ultimately need to be sacrificed. The DMSO controls were used to ensure that any phenotype exhibited by the MTZ treatment was solely caused by the drug and to ensure that in DMSO *Tg(NTR)* and WT fish responded equally well. The H_2O control group was used to ensure that DMSO did not cause any defect during the regenerative process.

In the first trial fish in all groups were anaesthetized and had their caudal fin amputated using the standard cut technique described above. At 3 days post amputation (dpa), which is when the first joint appears (Cardeira et al., 2016), fish were placed into their treatment or control solutions for 24 hours. After the treatment, *Tg(NTR)* fish in the experimental group treated with 10 mM MTZ still had joints forming in their regenerating fin distal to the amputation (Figure 3.2.1). This was confirmed by not only the presence of joints, but the presence of joint cells still expressing YFP. The length of bone segments between the experimental and control groups appeared similar in length.

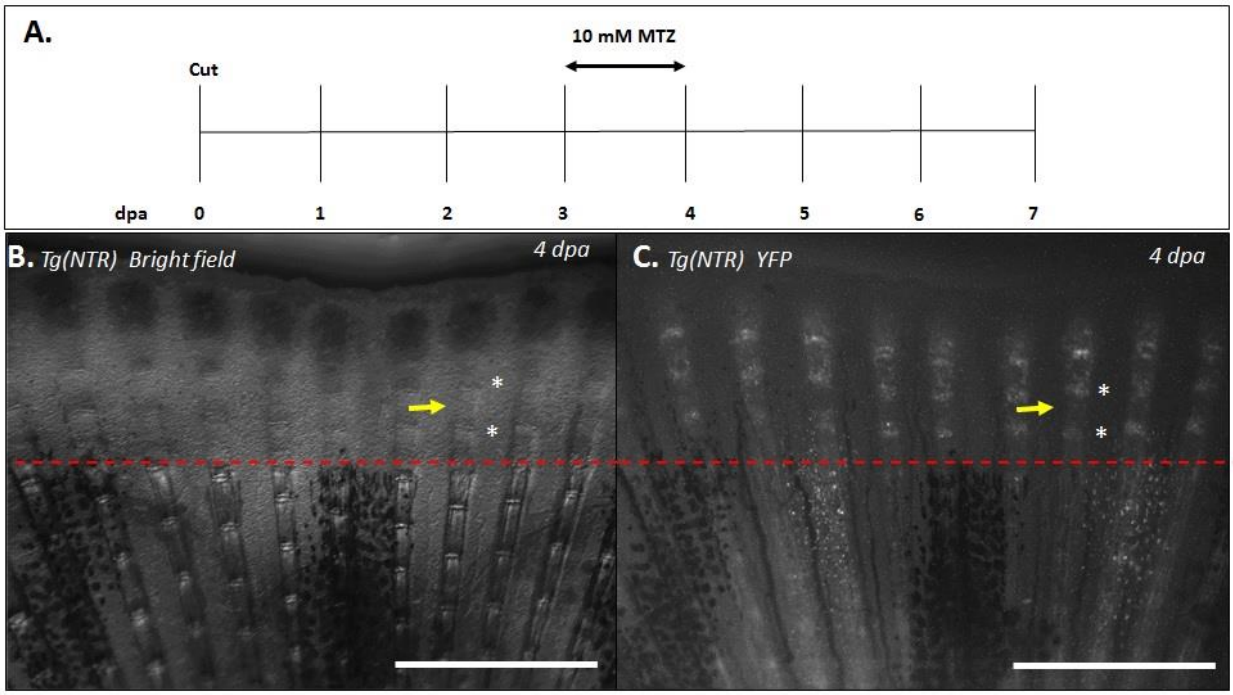

Figure 3.2.1 Time course and results of the first metronidazole trial: No loss of joints in the regenerate

The first MTZ treatment time course ran for 24 hours (**A**, black double-headed arrow) starting at 3 dpa, followed by the collection of images at 4 dpa. (**B**) Bright field images revealed that joints still formed during regeneration (white asterisks) separated by bone segments (yellow arrow) that appeared normal in length. (**C**) Under YFP UV filter the presence of joint cells was confirmed (white asterisks) verifying that newly formed joint cells were not eliminated during the experiment. Scale bars are 1mm.

This experiment was repeated but fish were left in MTZ for 30 hours beginning at 3 dpa in hopes a longer treatment period would ablate the joint cells. Under the YFP filter before 30 hours MTZ treatment the expression levels of YFP in *Tg*(*NTR*) fish were similar (Figure 3.2.22). After the treatment, there was a decrease in expression of YFP in *Tg*(*NTR*) fish treated with MTZ compared to DMSO control (Figure 3.2.2). This indicated that the longer treatment was ablating cells, but still not all of the cells were able to be ablated.

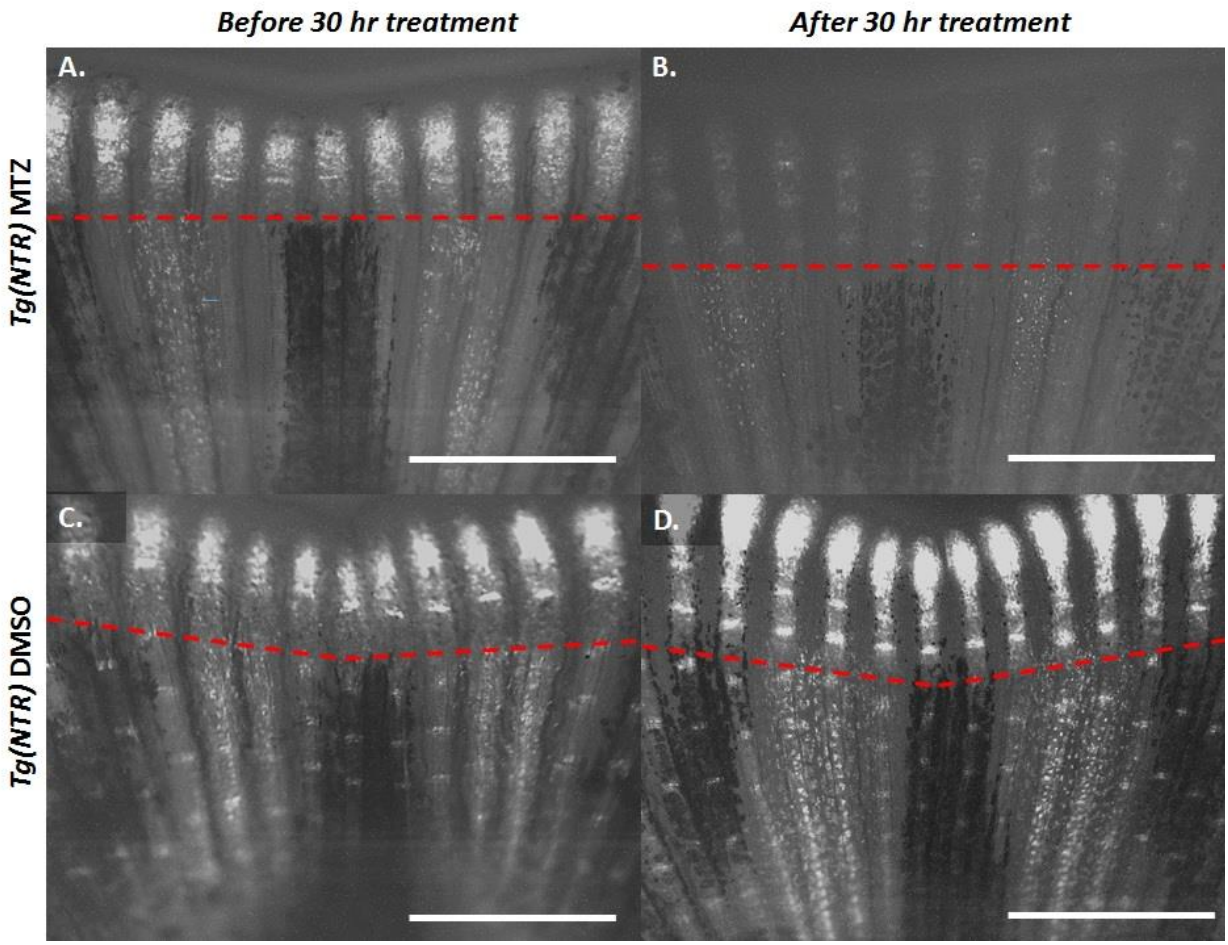

Figure 3.2.2 30-hour metronidazole treatment leads to reduction in YFP expression in *Tg(NTR)* fish

When the *Tg*(*NTR*) fish were treatment with 10 mM MTZ at 3 dpa for 30 hours there is a reduction in the expression levels of YFP (**A**-**B**) when compared to *Tg*(*NTR*) treated with DMSO (**C**-**D**). Scale bars are 1 mm.

In an attempt to remedy the failure to successfully eliminate joints during regeneration, the next trial was begun at 2.5 dpa which is before the first joint is formed in order to eliminate the joint cells as they are forming. Instead of 24 hours in MTZ, fish were left in the solution for 30 hours to allow MTZ to penetrate into the cells for a longer period of time (Figure 3.2.3A). The experimental and controls groups as well as number of fish per group remained the same. After the standard amputation of each fish, they were placed into their respective treatments for the 30 hours. After the treatment, all fish were moved to

system water and monitored up to 7 dpa. Once again, the joints still managed to form distal to the amputation.

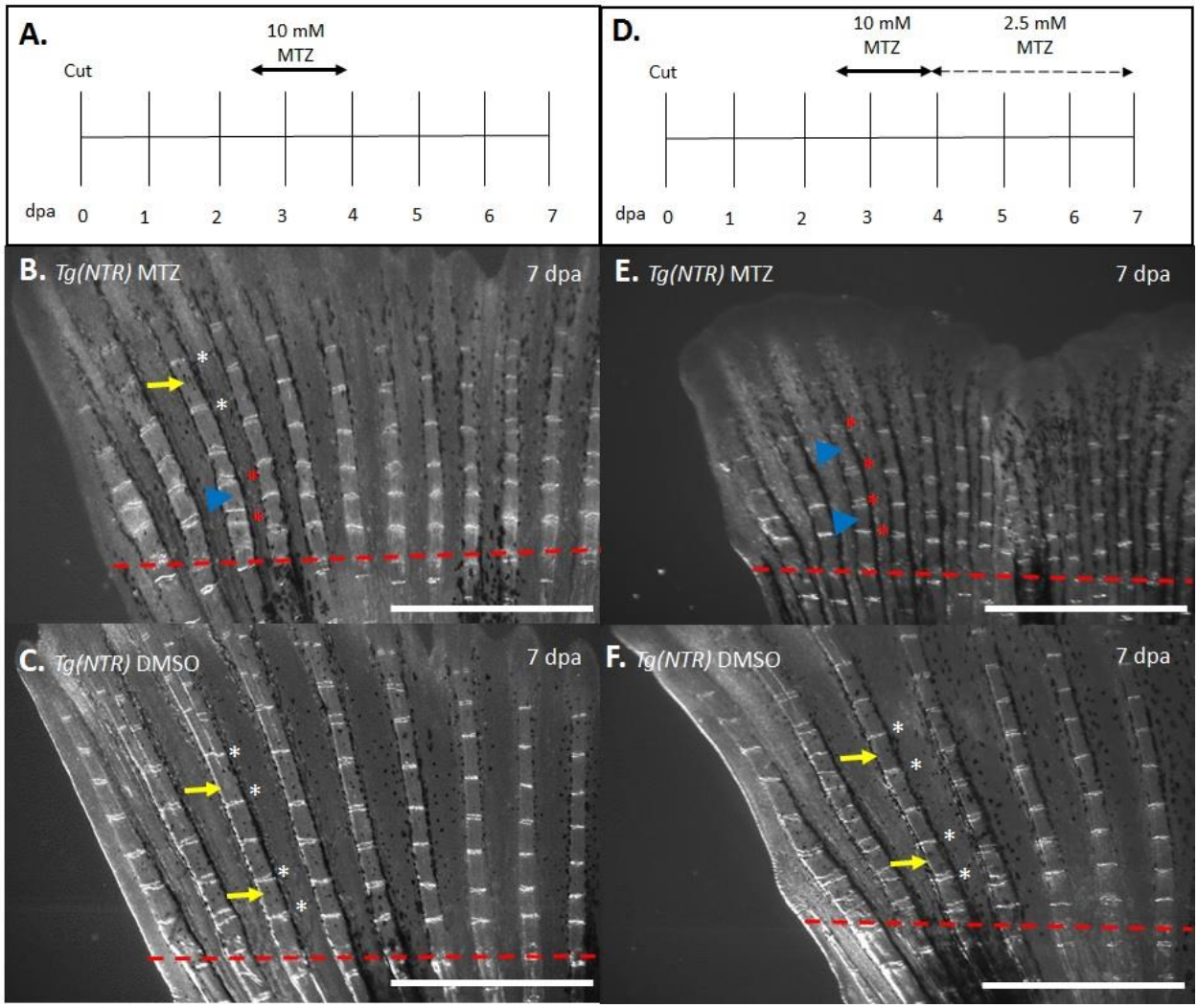

Figure 3.2.3 Constant presence of metronidazole resulted in disrupted joint development.
The MTZ treatments were begun at the 2.5dpa time point in an attempt to ablate cells as they formed (**A**). This did not result in fin regenerate that lacked joints, but did result in a disruption of the joints that formed during 30 hours spent in MTZ (red asterisk) and shortened bone segments (blue arrow). After the MTZ treatment was over subsequent bone segments (yellow arrow) and joints (white asterisk) returned to normal (**B**) when compared to the DMSO controls bone segments (yellow arrow) and joints (white asterisk) (**C**). The protocol was adjusted again so that after the initial 10 mM MTZ treatment fish were placed in 2.5mM MTZ for the remainder of the experiment (**D**). This did not eliminate joint formation during regeneration, it did however result in a continuation of the phenotype observed in the 30 hour 10mM MTZ that manifested itself with shortened bone segments (blue arrows) and disrupted joint formation (red asterisks) (**E**) when compared to the bone segments (yellow arrow) and joints (white asterisks) of the controls (**F**). Scale bars are 1mm.

Despite the joints still forming, the first 3 joints that formed were notably different from the first three joints in the control group. The joints did not appear to be as perpendicular to the fin ray as they appeared in all the control joints (Figure 3.2.3). The bone segments that separated the first three joints were not as long as they were in the control groups. Sister hemirays of these shortened bone segments also did not appear to line up with each other as well as in controls where the joints side by side, instead the joint formations were staggered between the sister hemirays. Joints that formed after the treatment regained their regular appearance and spacing between joints. Although there was a disruption in joint formation, there was no success in eliminating the formation of any of the new joints during regeneration.

The protocol was altered once again in an attempt to eliminate the formation of new joints during regeneration. The 30 hours treatment period was kept however after the 30 hours in 10 mM MTZ, *Tg(NTR)* and WT control were placed into 2.5 mM MTZ until 7 dpa (Figure 3.2.3D). This was an alteration of a protocol used by Petrie *et al* (2014) in which they kept their nitroreductase transgenic fish in 2.5 mM MTZ for the entire experiment and had around 90% cells ablation. Even with this amendment to the treatment the joints of the *Tg(NTR)* MTZ fish still appeared in the regenerate. Once again, the first 3 joints of the *Tg(NTR)* MTZ that formed in the 30-hour 10 mM MTZ treatment were disrupted as before. This phenotype now continued in the joints that formed in the 2.5 mM MTZ treatment, characterized by joints that were not perpendicular to the fin ray, shortened bone segments, and staggered joints that did not line up. From this point onward when MTZ treatment is referred to it will be the treatment course in Figure 3.2.3D.

To determine if there was a significant reduction in the length of the segments that formed in the regenerate of the *Tg(NTR)* fish treated with MTZ compared to controls in fish that underwent the MTZ treatment seen in Figure 3.2.3D, the first three segments and the total regenerative length after 7 dpa of the three most dorsal bifurcated fin rays were measured and compared between *Tg(NTR)* MTZ, *Tg(NTR)* DMSO, and WT MTZ fish (Figure 3.2.4). The first segment, which is measured from the first joint formed distal to the amputation to the second joint. The Mann-Whitney test showed there was a significant difference between *Tg(NTR)* MTZ and *Tg(NTR)* DMSO ($p = <0.05$) and a significant difference between *Tg(NTR)* MTZ and WT MTZ ($p = <0.05$) (Figure 3.2.4A). The second segment, which is measured from the second formed joint to the third. The Mann-Whitney test showed there was a significant difference between *Tg(NTR)* MTZ and *Tg(NTR)* DMSO ($p = <0.05$) and a significant difference between *Tg(NTR)* MTZ and WT MTZ ($p = <0.05$) (Figure 3.2.4B). The third segment, which is measured from the third formed joint to the fourth. The Mann-Whitney test showed there was not a significant difference between *Tg(NTR)* MTZ and *Tg(NTR)* DMSO ($p = >0.05$) and a significant difference between *Tg(NTR)* MTZ and WT MTZ ($p = <0.05$) (Figure 3.2.4C). The overall length of the regenerate gave an p-value >0.05 in each comparison.

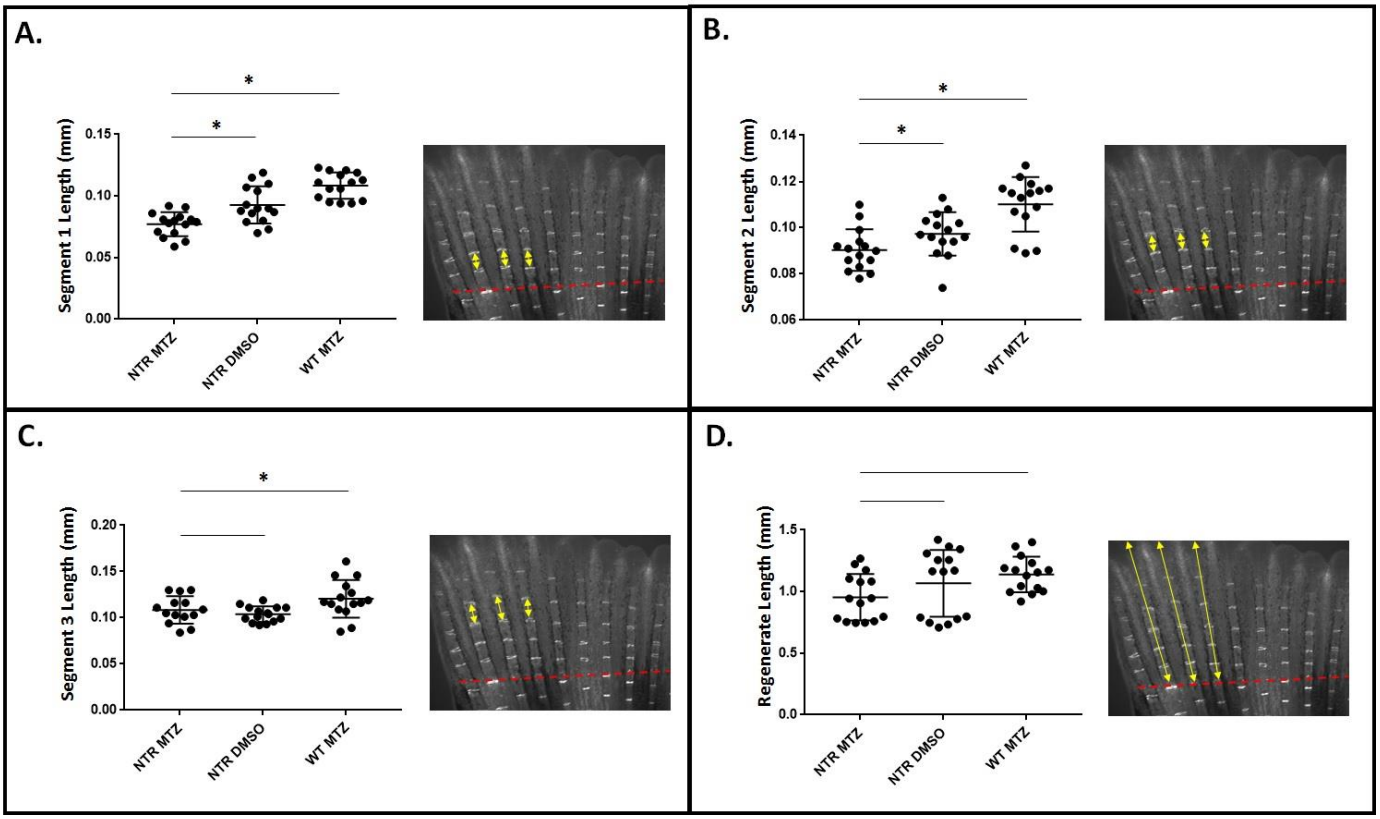

Figure 3.2.4 Bone segments of *tg(NTR)* that form earlier in regeneration are reduced in length when treated with MTZ

A significant difference was found between the length of *Tg(NTR)* MTZ segments and controls for the first and second segment (**A,B**). The third segment (yellow double headed arrows) did not have a significant difference in the length between *Tg(NTR)* MTZ and *Tg(NTR)* DMSO, but a significant difference was seen between *Tg(NTR)* MTZ and WT MTZ(**C**). The total length of the regenerate also did not show a significant difference between groups (**D**). * indicates significance. Data collected from experimental trials, each containing 3 fishes per group. * denotes p-value <0.05.

Next, we wanted to determine if there was an increase in cell death that could be causing the reduction in the length of the forming bone segments. If our NTR/MTZ system was working as we had theorized then joint cells should be dying in the presence of MTZ which could lead to the reduction in bone segment length. To determine if this was occurring, a TUNEL assay was performed on longitudinal sections of fins which labels cells undergoing apoptosis, the type of death that would occur in these cells. This was performed at 7 dpa on fish that had undergone the most recent MTZ treatment (Figure 3.2.3D) as this group was believed to have the most likelihood of joint cells undergoing apoptosis. Sections were

created from 3 different fins within each group, the best quality sections were examined for TUNEL positive cells. The best quality and most representative section for the TUNEL positive sections from each group were then imaged using a confocal microscope (Figure 3.2.5). Cells were counted manually in the entire section twice a week apart and the totals averaged in an attempt to eliminate human error.

In the *Tg(NTR)* DMSO and WT MTZ fish TUNEL positive cells were scattered throughout various tissue, appearing primarily in the epidermis and mesenchyme (Figure 3.2.5C-D). The *Tg(NTR)* DMSO sections had an averaged total of 30 TUNEL positive cells while the WT MTZ sections had an averaged total of 33 TUNEL positive cells. The *Tg(NTR)* MTZ had a total of 82 TUNEL positive cells throughout the entire section. Upon closer inspection, the cells appeared to be scattered throughout the epidermis and mesenchyme as was seen in the controls, but was also seen in the area of the proximal blastema and in the actinotrichia-forming cells (Figure 3.2.5A). These TUNEL positive cells are where the *Inta11* regulatory elements drive expression, indicating that this increase in TUNEL positive cells could be due to the MTZ treatment. The cluster of cells seen on the left side of the section appear more internal than the osteoblasts, suggesting they may be actinotrichia-forming cells. This experiment will need to be repeated so that statistically relevance can be calculated.

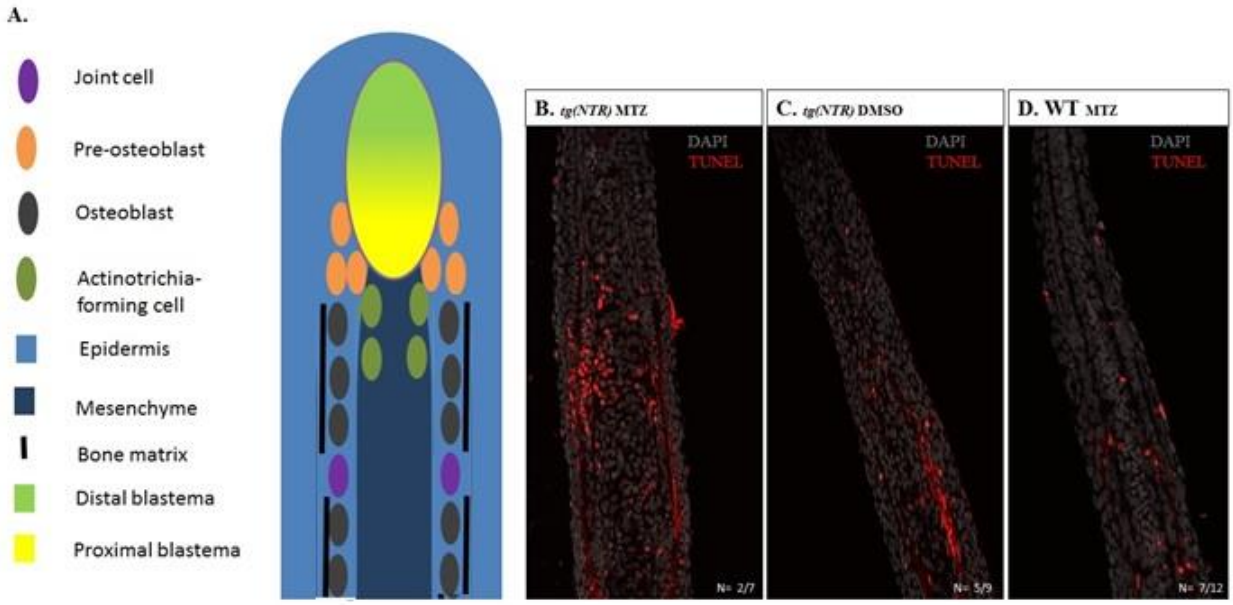

Figure 3.2.5 Metronidazole treatment showed increase in TUNEL positive cells *Tg(NTR)* fish.

TUNEL was performed on longitudinal sections of *Tg(NTR)* MTZ, *Tg(NTR)* DMSO, and WT MTZ fins at 7 dpa to detect apoptosis. (**A**) Cartoon longitudinal sections shows the various cell and tissue types. (**B**) In *Tg(NTR)* MTZ fin sections there were more TUNEL positive cells (82 total) than in controls, and TUNEL positive cells were found in a wider variety of tissus including a cluster of positive cells that may constitute actinotrichia-forming cell. (**C,D)**In *Tg(NTR)* DMSO and WT MTZ sections TUNEL positive cells (30 and 33 respectively) were scattered throughout the epidermis and mesenchyme. N = number of TUNEL positive sections of out intact sections examined.

At this point we had found that MTZ treatment led to shorter bone segments and that there was also an increase in apoptotic cells in the fish that had shown this phenotype. This however did not answer the question of why we were unable to completely eliminate joints from forming in the regenerate. There were two main ideas of why we were unable to completely eliminate the joints; the first was that not enough MTZ was getting into the cells or the NTR levels were not sufficient enough to reduce the MTZ, the second was that given their incredibly fast regenerative capabilities the zebrafish were replacing apoptotic cells faster than the NTR/MTZ system could ablate them. With the latter being easier to detect

we decided to perform a PCNA assay on longitudinal fin sections to examine cell proliferation in the same area we saw an increase in cell death.

The blastema is the highly proliferative group of cells found in the fin regenerate, and in Figure 3.2.6A-C the majority of PCNA positive cells appear in this region within each section along with additional positive cells scattered throughout the epidermis and mesenchyme. Longitudinal sections were created from three different fins from each group; *Tg(NTR)* MTZ, *Tg(NTR)* DMSO and WT MTZ. All PCNA positive cells on the sections were counted twice manually a week apart and averaged where applicable in an attempt to eliminate human error. The *Tg(NTR)* MTZ fin sections had an averaged total of 103 PCNA positive cells (Figure 3.2.6A). The *Tg(NTR)* DMSO and WT MTZ controls had 135 and 97 positive cells respectively (Figure 3.2.6 B-C). Although the WT MTZ had less PCNA positive cells than the *Tg(NTR)* MTZ, this is explained through the poor quality of the sections on the slide after the PCNA treatment, what is shown in Figure 3.2.6C constitutes the best-preserved section of the WT MTZ sections. Since there wasn't enough sections to run a statistical analysis, we cannot say in confidence that the MTZ treatment reduced proliferation in *Tg(NTR)* MTZ.

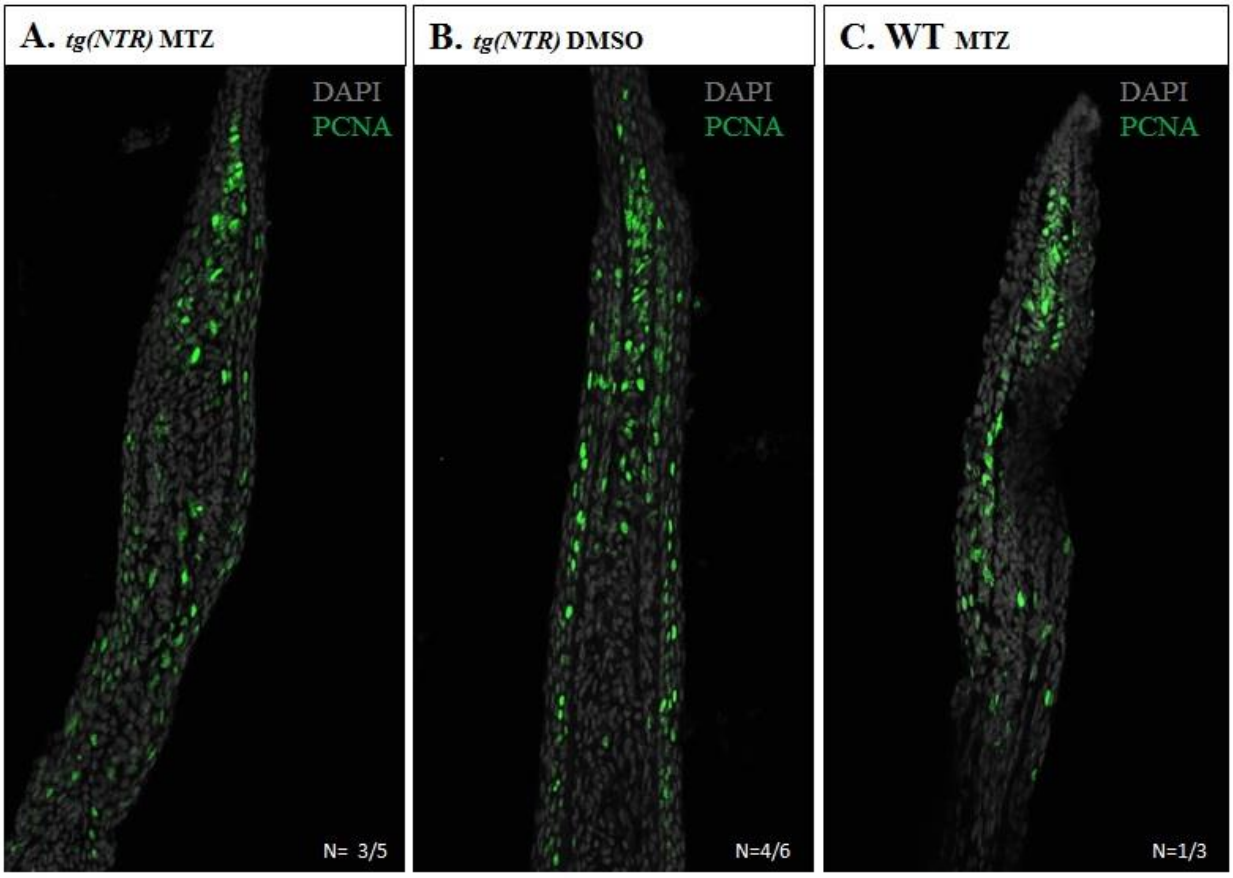

Figure 3.2.6 Proliferation in *Tg(NTR)* fish after metronidazole treatment.
PCNA was performed to detect proliferating cells in the blastema and surrounding proximal area of *Tg(NTR)* MTZ, *Tg(NTR)* DMSO, and WT MTZ fish at 7 dpa. The *Tg(NTR)* MTZ fish appeared to have a decrease in the amount of proliferating cells in the blastema and surrounding area (**A**) when compared to *Tg(NTR)* DMSO (**B**) and WT MTZ (**C**). N = PCNA positive sections out of the viable sections examined.

3.3 Metronidazole concentration gradient

Since the 10 mM MTZ treatment resulted in reduced bone segment length and a disruption of proper joint formation based on appearance in *Tg(NTR)*, we wanted to determine if incrementally increasing the concentration of MTZ would lead to an incremental decrease in segment length. 5, 10, and 15 mM MTZ increments were chosen for the initial 30 hours treatment period that began at 2.5 dpa, followed by 2.5 mM treatment up to 7 dpa. Not only was this to see if there was a correlation between MTZ concentration and

segment length, but to also see if a higher concentration could successfully eliminate the joints.

After the treatment, all of the *Tg(NTR)* MTZ treated fish were able to regenerate bone segments with newly formed joints. The 5 mM MTZ-treated *Tg(NTR)* did not appear to have greatly reduced bone segment length when compared to WT fish treated with the same concentration of MTZ. The newly formed joints in the *Tg(NTR)* 5 mM MTZ fish appeared disrupted as was seen previously denoted by their angled formation compared to the perpendicularly formed joints in the WT 5 mM MTZ control. This trend was also observed in both the 10 and 15 mM MTZ-treated *Tg(NTR)* fish when compared to their respective WT controls.

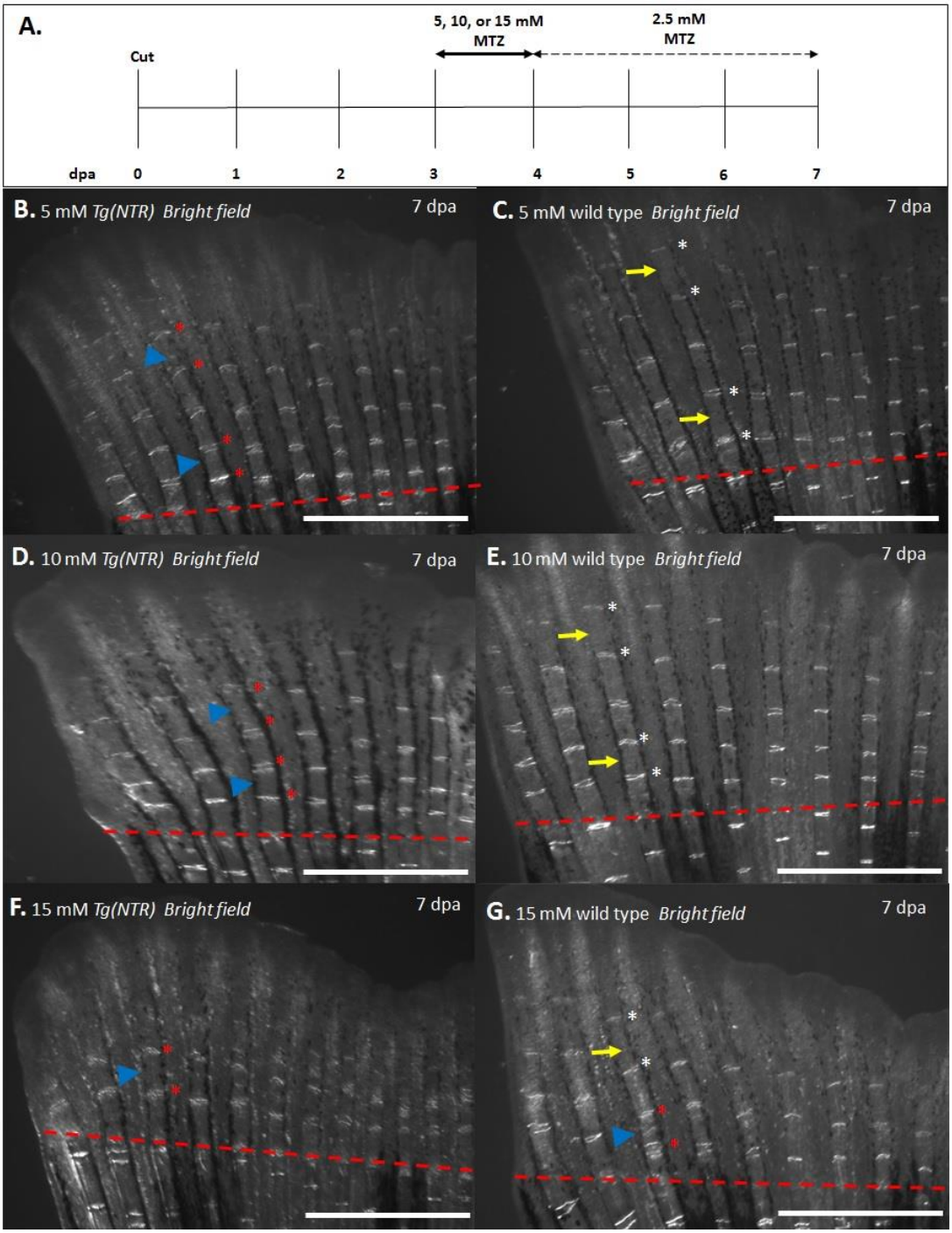

Figure 3.3.1 Metronidazole concentration gradient and corresponding bone segment length.

The concentration gradient followed the same time points during experimental procedure as used previously (**A**). 5mM *Tg(NTR)* MTZ fish appeared to have slightly disrupted joints that were not perpendicular to the fin ray (red asterisks) and bone segments seems to be shorter (blue arrow) in length (**B**) than controls which had normal looking joints (white asterisks) and bone segments (yellow arrow) (**C**). 10mM *Tg(NTR)* MTZ fish appeared to have further reduced bone segments (blue arrow) and joint formation between sister hemirays appeared to be staggered (red asterisks) (**D**) when compared to the 10mM WT MTZ control fish

which had normal appearing joints (white asterisks) and bone segments (yellow arrow)(**E**). 15mM *Tg(NTR)* MTZ fish had joints that were disrupted and appeared less sharp than typical joints (red asterisks). Bone segments appeared to be reduced in length (blue arrow) and the overall regenerate and number of joints appeared to be greatly reduced as well (**F**). In the 15mM WT MTZ fish, early forming joints (red asterisks) and bone segments (blue arrow) appeared to be malformed similar to the 15mM *Tg(NTR)* MTZ fish indicating defects caused by MTZ (**G**).

The 5, 10 and 15 mM MTZ-treated Tg*(NTR)* fish appeared to have a reduction in bone segment length when compared to their controls. To determine if there was a significant difference between the lengths of the bone segments in each concentration when compared to their controls and statistical analysis was conducted. Measurements of the 1st, 2nd, and 3rd segment of the first three fin rays were compared amongst the groups. Each of the 1st, 2nd, and 3rd segment of each fin ray was compared to the corresponding WT control group. The first segment of both the 5mM and 10mM MTZ-treated *Tg(NTR)* had a significant reduction in the measured length when compared the corresponding WT control (Figure 3.3.3A). In the 15mm MTZ-treated Tg*(NTR)* fish there was not a significant difference when compared to the 15mM WT fish (Figure 3.3.3A). Statistical results from the second segment were the same as the first in the 5 and 10 mm MTZ-treated Tg*(NTR)* fish as a significant reduction when compared to their respective controls (Figure 3.3.3B). The 15mm MTZ-treated Tg*(NTR)* fish also had a reduction in length that was significant compared to its control in the second bone segment (Figure 3.3.3B). The third segment failed to reach a mature enough form in 15mm MTZ-treated Tg*(NTR)* fish where measurements could be performed reliably, so significance could not be determined. In both the 5mM and 10mm MTZ-treated Tg*(NTR)* fish there was once again a significant difference in the length of the bone segment (Figure 3.3.3C). The overall trend that was observed for the concentration gradients and segment length was that as concentration of MTZ increases in *Tg(NTR)* fish, the length of the bone segments decreases.

The total length of the regenerate in the 10 and 15 mm MTZ-treated Tg*(NTR)* fish appeared noticeably reduced in length when compared to the respective WT control group. Once again this was a trend that was not obvious in the 5 mm MTZ-treated Tg*(NTR)* fish when compared to its WT. To determine if there was a significant difference in the lengths of the regenerate measurements were taken for the standard fin rays used and *Tg(NTR)* were compared against their controls. The 10mM and 15mm MTZ-treated Tg*(NTR)* fish did have a significant difference in the length of their regenerated tissue compared to their WT controls (Figure 3.3.3D). 5mm MTZ-treated Tg*(NTR)* fish however did not have a significant reduction in the length of the regenerate when compared to the WT control after 7 dpa (Figure 3.3.3D).

It was noticed in WT fish the distance from the amputation site to the first joint that forms during regeneration appeared to be at a relatively similar distance regardless where the first joint proximal to the amputation site appears (Figure 3.3.2).

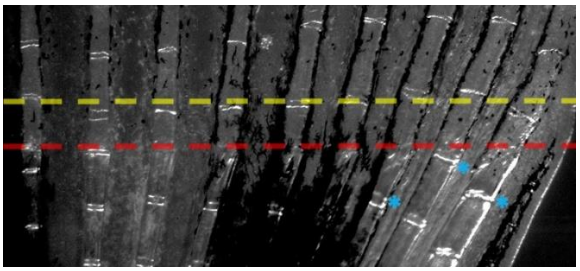

Figure 3.3.2 First joint during regeneration appears at consistent distance from cut site.
The distance from the amputation (red dashed line) to the first forming joint during regeneration (yellow dashed line) appears in at a similar distance regardless of last proximal joint location (blue asterisks).

We wanted to determine if ablating cells expressing *hoxa13a* in *Tg(NTR)* fish would result in a change in distance from cut site to first formed joint when compared to controls. In 5mM

and 10mm MTZ-treated Tg*(NTR)* fish the first joint formed significantly closer to the amputation site compared to the controls (Figure 3.3.3E). The 15mm MTZ-treated Tg*(NTR)* fish did not form at a distance from the amputation site that was significantly different than the 15mM WT control (Figure 3.3.3E).

It was also observed that between the different *Tg(NTR)* concentration groups, there seemed to be an inconsistent number of joints that formed after 7 dpa. The 5 mM had a similar number of joints that formed compared to the control. The 10 mm MTZ-treated Tg*(NTR)* fish had less than both its control and the 5 mm MTZ-treated Tg*(NTR)* fish, while the 15 mm MTZ-treated Tg*(NTR)* fish was drastically reduced in number of joints formed when compared to any of the groups. Statistical tests were performed to determine if there was a significant difference between the number of joints between *Tg(NTR)* fish and their WT controls, however there was no significant difference between *Tg(NTR)* and WT regardless of concentration (Figure 3.3.3F). The WT 15 mM MTZ control also appeared to have less joints than the 5 and 10 mM MTZ controls, this is likely due to the high concentration of MTZ causing defects during regeneration.

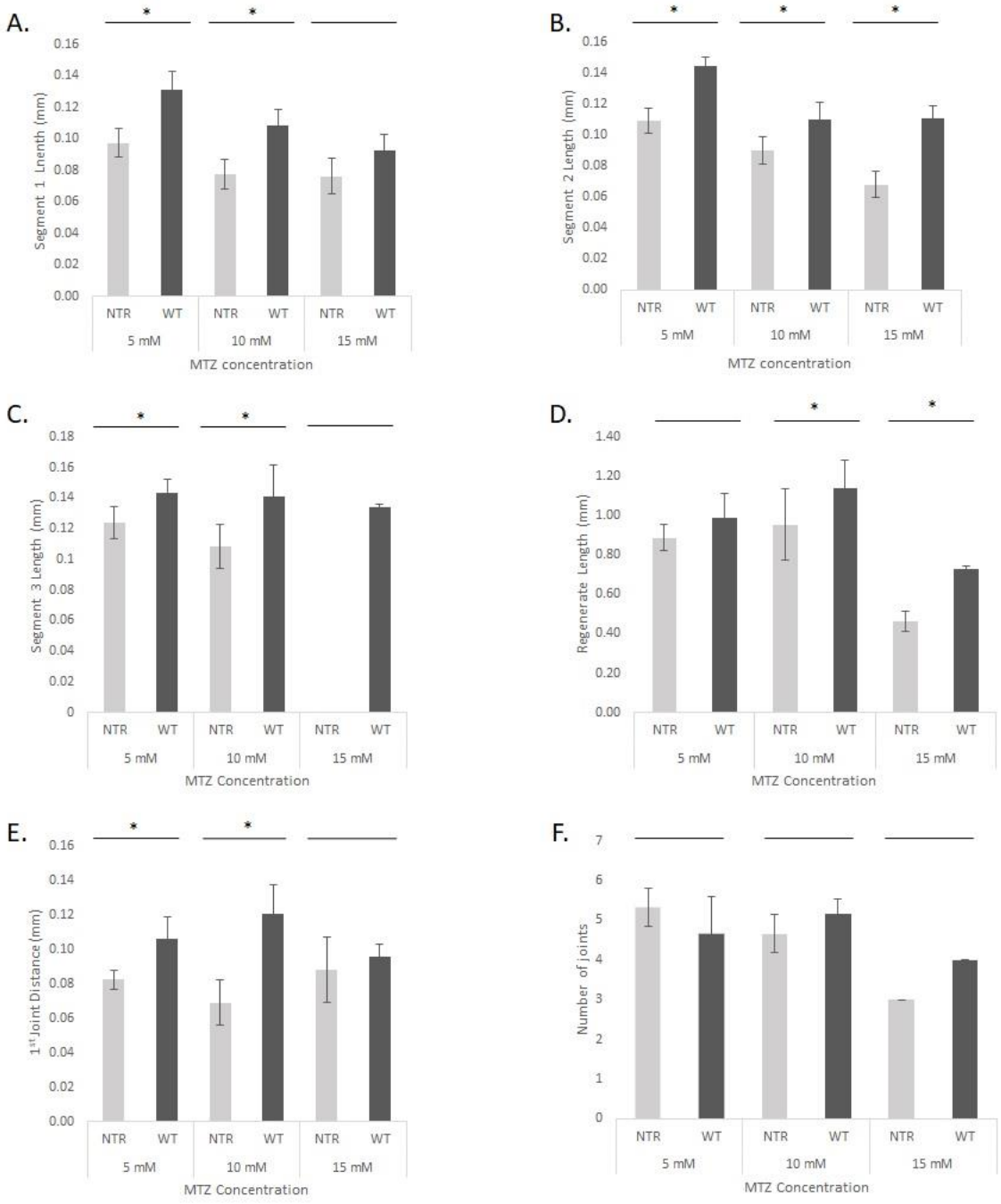

Figure 3.3.3 MTZ concentration gradient statistics for bone segment lengths, regenerate length and 1st joint distance from cut site.

Bone segment length was compared between *Tg(NTR)* MTZ and their WT MTZ controls to determine if there was a significant difference in length. (**A**) The first bone segment of 5 and 10mm Tg*(NTR)* MTZ was significantly shorter than the respective WT MTZ controls, while 15mM *Tg(NTR)* MTZ had no significant difference between length. (**B**) This patterned continued through the second bone segment however there was a significant difference in segment length between 15mM *Tg(NTR)* MTZ and 15mM WT MTZ fish. (**C**)The third bone segment of 5 and 10mM *Tg(NTR)* MTZ was significantly shorter than the respective WT MTZ controls and was not measureable in 15 mM *Tg(NTR)* MTZ as a third bone segment had not formed by 7 dpa. (**D**)Overall length of the fin regenerate was compared between tg*(NTR)* MTZ and WT MTZ controls. 10mM and 15 mM *Tg(NTR)* MTZ fish had a significant difference in the total length compared to controls while

5mM *Tg(NTR)* MTZ fish did not. (**E**) The distance from the cut site to the first formed joint was measured and found that the first joint formed significantly closer in 5mM and 10mM *Tg(NTR)* MTZ fish than their controls, however no difference was observed in 15mM *Tg(NTR)* MTZ fish and controls. (**F**) The number of joints that formed in the regenerate was determined for each *Tg(NTR)* MTZ concentration, however there was no significant difference between experimental and control groups. All data collect from the three most dermal bifurcating fin rays. Data for 5 and 10 mM *Tg(NTR)* MTZ and WT MTZ groups collected from 6 different fish. 15 mM *Tg(NTR)* MTZ and WT MTZ group contained 2 fish. All statistics generated from Mann-Whitney test. * denotes significance. Error bars represent standard deviation. * denotes p-value <0.05.

After comparing the MTZ concentration groups to their controls, they were compared to one another to determine if increasing concentration lead to decreasing bone segment length. Comparisons using the Mann-Whitney test showed there was a significant difference between first segment length of 5 mM and 10 mM as well as between 5 mM and 15 mM (Figure 3.3.4). Comparison using the Mann-Whitney test showed there was a significant difference between second segment length of all groups compared (Figure 3.3.4). The 15 mm MTZ-treated Tg(*NTR*) fish did not develop a measurable third bone segment after 7 dpt, so the Mann-Whitney test was used to compare the third bone segment of 5 and 10 mM, where a significant difference was found.

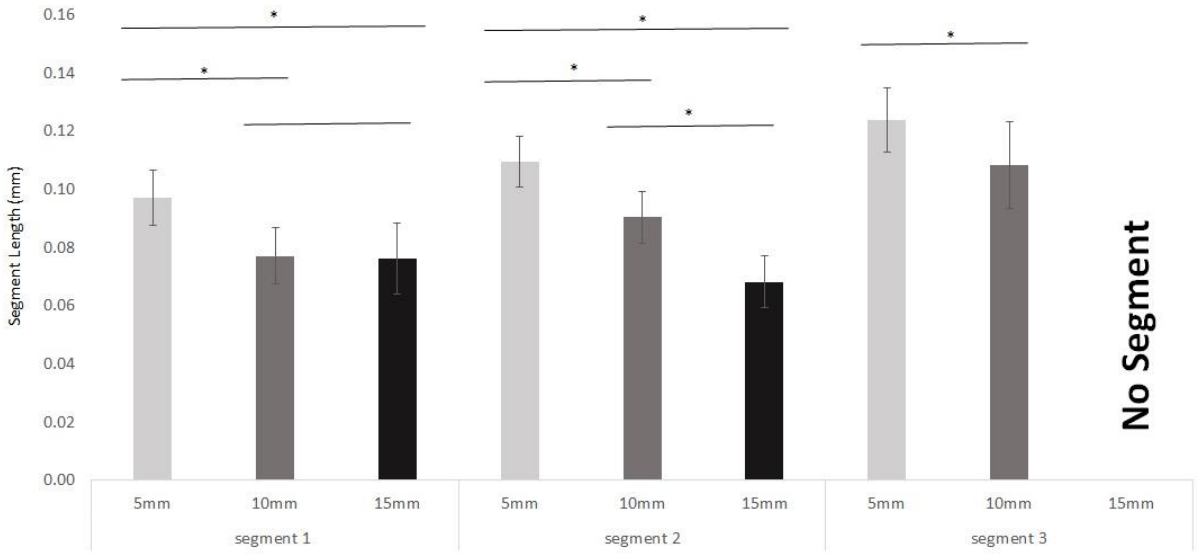

Figure 3.3.4 Statistics show increasing MTZ concentration results in shorter bone segments

The length of the first three segments of the difference concentrations of MTZ (5, 10, and 15 mM) were compared against each other to determine if there was a significant difference the lengths in relation to their concentrations. The 5 mM treated *Tg(NTR)* fish had significantly longer bone segments than both 10 and 15 mM *Tg(NTR)* fish in every measurement in which they were comparable. The 10 mM *Tg(NTR)* fish bone segments only differed significantly in the second segment when compared to 15 mM *Tg(NTR)* fish. * denotes p-value <0.05.

4 Discussion

The goal of my project was to eliminate the joint cells during fin regeneration in adult zebrafish and determine if this would lead to a regenerate completely lacking joints. To accomplish this two methods were used. We first utilized the NTR/MTZ chemo-ablation technique in which MTZ would lead to apoptosis in cells that expressed NTR. The cells that were targeted were presumptive and committed cells that expressed *hoxa13a*. The expression of *hoxa13a* has been shown to be required for proper joint development in zebrafish, but its role in joint formation during regeneration is a novel area of study (Nakamura *et al*, 2016). The second method involved creating transgenic fish lines that

would ectopically express cell fate commitment markers and entice common lineage cells to become either osteoblast or joint cells. It is believed that by controlling spatial and temporal expression of known and hypothesized runx2^{+} cell fate commitment markers we will be able to cause a regenerate to form without joints and without osteoblasts.

4.1 Metronidazole treatment fails to completely eliminate joints cells during regeneration

The *Tg(Inta11-β-globin:YFP-2A-NTR)* transgenic fish used in the MTZ experiments did not successfully have their joints eliminated during the 7 dpa treatment period. A phenotype was observed after treatments that manifested itself as shortened bone segments and disrupted joint formation. There was also an increase in TUNEL positive cells after 7 dpa in *Tg(NTR)* fish treated with MTZ. The expression of NTR was driven by *Inta11* regulatory element, which is activated by *hoxa13a* as shown previously (Kherdjemil et al., 2016; Lalonde, manuscript submitted 2017) and drives expression in presumptive, committed, and mature joint cells, actinotrichia forming cells and possibly the blastema (Figure 3.1.1).

PCNA assay results suggested that there was not an increase in proliferation in cell types that were targeted for ablation, instead have shown that there may be less proliferation in *Tg(NTR)* fish treated with MTZ than in controls, specifically in the blastema and in the proliferating osteoblast cell lineage (Figure 3.2.6). When PCNA positive cells were counted the *Tg(NTR)* DMSO treated fish had over 30% more positive cells than the *Tg(NTR)* MTZ fish. The WT MTZ and *Tg(NTR)* MTZ were comparable in number of PCNA positive cells, but this was most likely due to the poor quality of even the best section after the protocol was complete. Statistical was not conducted due to a low number of available sections.

Since the *Inta11* regulatory elements drive expression in both the pre-osteoblast cells where the presumptive joints form, the actinotrichia-forming cells and possibly the blastema, all of which are areas where proliferation may have been reduced, it is difficult to determine to what extent the loss of proliferation in each group of cells contributes to the phenotype observed. Studies have shown that blastema proliferation is at least partially controlled by the notch signaling pathway (Münch et al., 2013). When the notch pathway is completely inhibited, fin regenerates fail to form, however in MO knockdown of *notch1b* there is a sizable reduction in proliferation within the blastema that results in a stunted regenerated fin (Münch et al., 2013). This reduction in the fin regenerate was more pronounced than what was observed in the phenotype of the *Tg(NTR)* fish treated with MTZ, but the reasoning is likely that the MO knockdown of *notch1b* appeared to cause a greater reduction in proliferation than we observed because it is directly involved in blastema proliferation. However, the effects observed in the *Tg*(*NTR*) fish treated with metronidazole is not limited to decreased proliferation in the blastema, there is also a reduction in bone segment length. Shortfin genetic mutant zebrafish (sof^{b123}) exhibit both shorten bone segments and shorten fin length compared to wild type fish due to a decrease in *connexin 43* (*cx43*), a subunit of connexons (Sims, Eble, & Iovine, 2009). Connexons are assembled protein complexes that allow for the exchange of small molecules between cells. These complexes are embedded in the cell membrane and two connexin complexes from neighboring cells create a protein channel, also called a gap junction (Iovine et al., 2005). In the regenerating zebrafish fin, *cx43* expression is present in both the joint cells and blastema. Reduction in this expression leads to reduced length of both bone segments and total fin regenerate (Hoptak-Solga et al., 2008; Iovine et al., 2005).

Although joint cell death was not directly observed in the TUNEL assay, there was an increase in apoptotic cells in the pre-osteoblast cells from which joint cells are derived as well as within the blastema of *Tg(NTR)* fish treated with MTZ (Figure 3.2.5). Images taken under the YFP filter show a reduction in the amount of YFP seen around the joints in *Tg(NTR)* fish treated with MTZ after 30 hours compared to *Tg(NTR)* DMSO fish (Figure 3.2.2). This suggested that joint cells were being ablated but not at a level sufficient enough to completely eliminate joints. Based on the results from an embryonic stage ablation of *hoxa13a* expressing cell using the same transgenic line, we were able to deem it highly unlikely MTZ was causing necrosis in cells at the concentrations used in our experiment.

These results agree with a previously proposed simulated mechanism for joint patterning during regeneration in which joint cells produce a joint-inhibiting molecule to ensure that, in the immediate area surrounding a joint, no other joint will form until levels of the inhibiting molecule is reduced (Rolland-Lagan et al., 2012). It is reasonable to assume that if there is a reduction in the number of presumptive joint cells that remain after the MTZ treatment, this would reduce the amount of joint-inhibiting molecule that is being synthesized. This relief of joint cell commitment inhibition would then allow the proceeding joint to form earlier than it typically would, resulting in reduced distance between joints (shorter bone segments).

Alternatively, since TUNEL revealed that cells within the *runx2a* domain have an increase in apoptosis, this could be an explanation of why we saw a significant reduction in bone segment length in the *Tg(NTR)* 10 mM MTZ fish. The reduction in bone segment length could in turn be the cause for the significant reduction in regenerate length since the

number of joints between *Tg(NTR)* fish treated with MTZ than *Tg(NTR)* DMSO control is not significantly different.

4.2 Results of metronidazole treatments on Tg (*NTR*) fish fit with proposed joint forming models

The results obtained fit our proposed model for joint formation. In our proposed model, we suggest that once *runx2a* expressing cells commit to becoming joint cells, the maturing cells will begin to synthesize a joint inhibitor. This will create a *hoxa13a* gradient where another cluster of presumptive joint cells will not be able to form until a certain threshold concentration of *hoxa13a* is reached. We also propose that the formation of the first joint occurs when the *hoxa13a* concentration hits a threshold concentration and that this initial introduction occurs shortly after blastema formation.

4.2.1 Distance from amputation site to first formed joint in Tg (*NTR*) fits proposed model

We noticed that upon amputation of the caudal fin, the first regenerated joint in each fin ray was formed at a similar distance from the wound regardless of where the joint proximal to the wound was (Figure 3.3.2). In our joint model we propose that *hoxa13a* concentration is an early initiating factor in joint commitment. The expression of *hoxa13a* after injury coincides with formation of the blastema. We have shown this through the upregulation of YFP expression in our *Tg*(*NTR*) fish lines where *Inta11*, activated by *hoxa13a* (Kherdjemil et al., 2016; Lalonde, manuscript submitted 2017), drives expression of YFP early in the regenerative process (Figure 3.1.1A). The expression of the *hoxa13* gene is also found during blastema formation and throughout limb regeneration in other species with regenerative capabilities, including *Xenopus* (Ohgo et al., 2010).

Our results have shown that *Tg*(*NTR*) fish treated with MTZ form the first joint distal to the wound at a significantly shorter distance than compared to controls (Figure 3.3.3). Preliminary results suggest that the MTZ treatments appear to reduce the amount of proliferation in the *runx2a* expressing and blastema cells. In previous studies reduction in blastema proliferation resulted in atypical fin patterning and/or reduced length of regenerate (Iovine et al., 2005; Münch et al., 2013; Simões et al., 2014) which is the same phenotype we have seen. Since *hoxa13a* is expressed in the early stages of regeneration, it is highly likely that we are killing blastema cells early on in the outgrowth stage as we were targeting the first forming presumptive joint cells beginning at 2.5 dpa. It is unclear to what degree ablating the cells of the blastema had on regeneration in the experiment, but growth appeared to be slowed down. At the same time the presumptive joint cells were being ablated, allowing the proceeding joint to develop in closer proximity than normal. It is possible that the death of these two groups of cells created a stacking effect where outgrowth was slowed down and the *hoxa13a* threshold required to form a joint was reduced, resulting in the first joint forming closer to the amputation site (Figure 4.2.1).

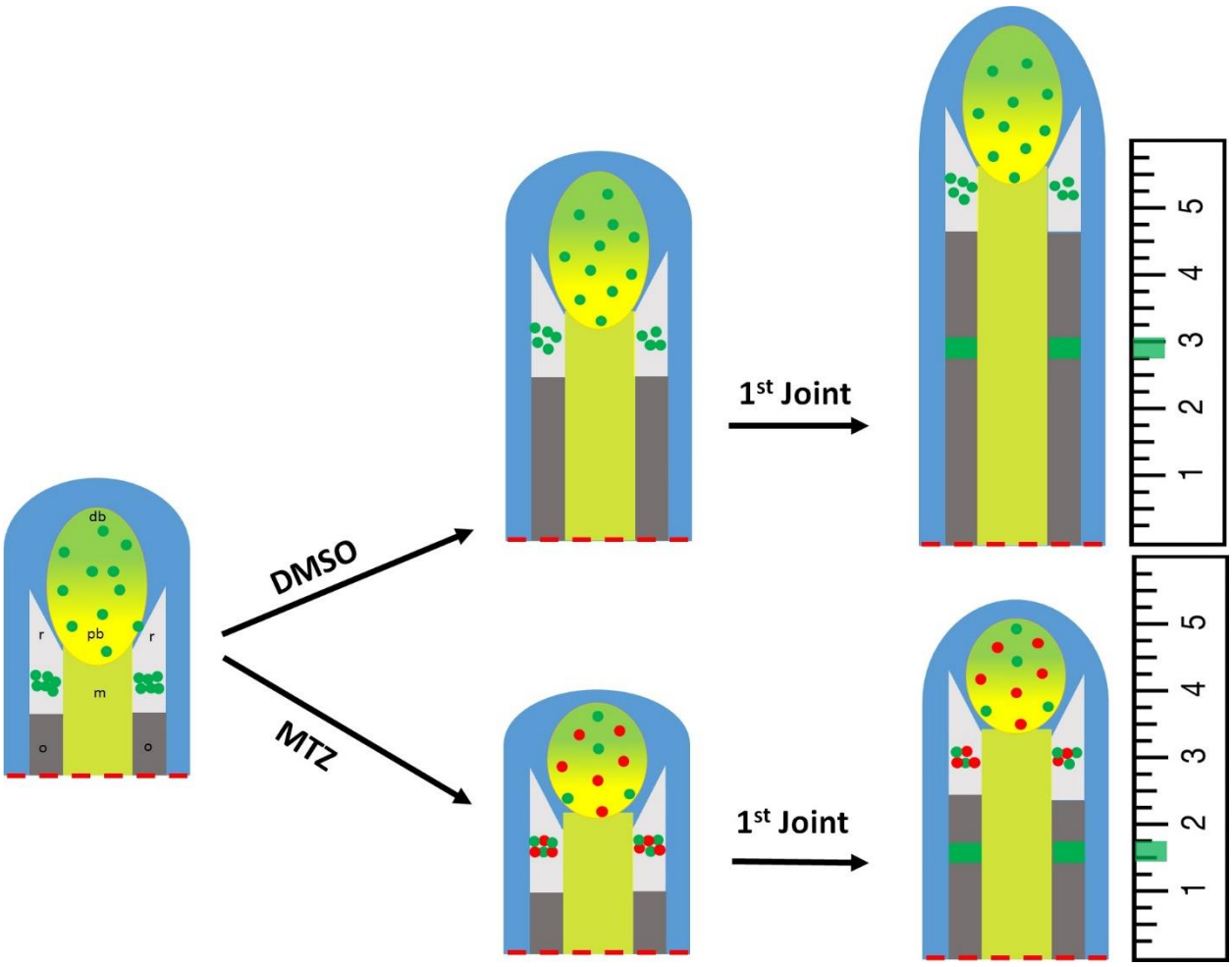

Figure 4.2.1 Reduced length of 1st joint in Tg(*NTR*) fish fits model
2.5 dpa Tg(*NTR*) fish are treated with DMSO or MTZ. In DMSO *hoxa13a* expressing cells in the *runx2a* (r) region reach the joint commitment threshold as the blastema continues with normal outgrowth giving rise to osteoblast (o) and mesenchymal (m) cells. In MTZ some of the *hoxa13a* expressing cells are ablated (red circles) as are cells in the distal and proximal blastema (db and pb) resulting in reduced outgrowth and 1st joint forming distance.

4.2.2 The observed phenotype in *Tg*(*NTR*) fit the proposed subsequent joint formation model

The first phenotype observed during fin regeneration in the *Tg*(*NTR*) fish treated with metronidazole was the regenerate had shortened bone segments and anomalous joint appearance. Although this difference in segment length was significant, it could not be determined whether it was due to joint cell ablation, suspected loss of proliferating cells in

the blastema, or a combination of the two. Regardless of which of the causes it may have been, the results still fit our proposed joint model. The proposed model stipulates that once *runx2a* expressing pre-osteoblasts cells commit to becoming joint cells, they begin to produce a joint inhibitor. As the regenerate continues to grow outward the joint cells mature and continue to express the inhibitor, whose concentration gets weaker in the *runx2a*-expressing pre-osteoblast cells as regeneration continues creating a gradient. Once the inhibitor level is low enough, *hoxa13a* hits a threshold in pre-osteoblasts committing a select few to become joint cells and the cycle repeats. If solely the joint cells were being ablating in our model, even if not completely as our data would suggest, then the concentration of the inhibitor would be weaker as less cells would be producing it. This in turn would lead to *hoxa13a* reaching its threshold in *runx2a* cells faster and the subsequent joint forming earlier. Although we also ablated *hoxa13a*-expressing cells, we believe that once the joint inhibitor is severely reduced, the pre-osteoblasts will reach the *hoxa13a* threshold quickly and induce early joint formation. The results have shown however that blastema proliferation is likely reduced in *Tg*(*NTR*) fish treated with MTZ which would decrease regenerate length as well as disrupt fin patterning (Simões et al., 2014) as we have seen. For this reason, it is likely that there is ablation of both joint cells and blastema cells during the experiment which is enhancing the effects that we are seeing.

Other studies of caudal fin regeneration have shown that disruption of the joint cells and blastema can lead to the phenotype we observed in the *Tg*(*NTR*) treated with MTZ. Quint *et al.* used cyclopamine treatments on regenerating zebrafish caudal fins to inhibit *sonic hedgehog* (*shh*) signal transduction at 2 dpa resulting in a reduction in blastema proliferation and eventually a decrease in regenerative length, interestingly however

segment length was not reduced (Quint et al., 2002). Similar results were found by Lee *et al*. whose group used inducible domain negative-*fibroblast growth factor receptor 1* (dn-*fgfr1*) transgenic fish to reduce *fibroblast growth factor* (*fgf*) expression, a growth factor, known for its role in the proliferative state of the blastema during regeneration (Kenneth D. Poss et al., 2000). The group found that when dn-*fgfr1* was expressed during regeneration and reducing *fgf* signaling, blastema proliferation decreased and shorter fin regenerate resulted, however bone segment length was normal (Yoonsung Lee, Grill, Sanchez, Murphy-Ryan, & Poss, 2005). In both of these cases blastema proliferation is disrupted as it appeared to be in the MTZ treatments, and the result in all three cases is reduced length of the fin regenerate, although bone segment length is not affected in the previously mentioned studies. This would suggest that joint cells are being ablated during the regenerative process in the MTZ treatments and that this is a likely cause for the reduction in bone segment length. Data regarding the ablation of immature joint cells during regeneration is much more limited. There have been no studies which chemo-ablate developing joint cells during regeneration, however studies have shown blocking downstream members of the joint formation pathway can eliminate joints. *Even-skipped 1* (*evx1*) is a transcription factor that has been shown to be required for joint formation not only during regeneration but in development as *evx1*$^{-/-}$ mutants develop fins with no joints (Schulte et al., 2011; Ton & Iovine, 2013). It has been suggested that *connexin43* (*cx43*) expression negatively regulates *evx1* expression shown through ISH of *evx1* after altering *cx43* expression (Dardis G, Tryon R, Ton Q, Johnson SL, 2017). When *cx43* expression was downregulated using a transgenic zebrafish sponge line to inducibly absorb the *miR-133a* which tags *cx43* for degradation, the *evx1* expression was decreased compared to

controls (Dardis G, Tryon R, Ton Q, Johnson SL, 2017). In a similar but opposite manner, overexpression of *miR-133a* which led to reduced levels of *cx43* resulted in increased expression of *evx1* compared to controls (Dardis G, Tryon R, Ton Q, Johnson SL, 2017). Based on data from our lab we have shown that *hoxa13a* is expressed in presumptive joint cells earlier than *evx1* and have found that *hoxa13a* is expressed in the *evx1*$^{-/-}$ mutants. If *hoxa13a* is upstream of *evx1* then it is entirely possible that *cx43* expression is actually reducing *hoxa13a* expression and the effect on the expression of *evx1* is a consequence of this. The zebrafish short fin mutant (*sof* ^{b123}) is characterized by reduced fin length, bone segment length, and cell proliferation caused by reduced levels of *cx43* mRNA and protein (Iovine et al., 2005). The phenotype was mirrored in fins of WT fish that underwent morpholino-mediated knockdown of *cx43* (Hoptak-Solga et al., 2008). The lifting of inhibition of *hoxa13a* through reduction of *cx43* expression is analogous to partially eliminating joints in our MTZ experiments based on our proposed model where inhibition would also be reduced. In both cases the result is a reduction of bone segment length in the fin regenerate. This in turn would suggest that a complete inhibition of *hoxa13a* expression during regeneration would lead to a regenerated fin without joints.

4.3 Increasing metronidazole concentration results in reduced bone segment length

Using 5, 10, and 15 mM MTZ concentrations we found that as concentration increases, the more pronounced the reduction in bone segment and regenerate length in *Tg*(*NTR*) fish becomes. This difference was most obvious when comparing 5 and 10 mM MTZ due to the fact that 15 mM MTZ failed to form a third bone segment after 7 dpa, which is most likely caused by non-specific effects of the high concentration of MTZ. The length of the first segment in 15 mM treated fish that formed was comparable to the first

10 mM segment, but the second was significantly shorter. It is unclear if this was due to joint cell death, blastema death, or non-specific effects (Curado et al., 2008). In WT fish treated with 15 mM MTZ there was disruption of the first regenerated joint noticed (Figure 3.3.1G). This non-specific effect combined with reduction in proliferation of the blastema is what most likely caused the drastic reduction in fin regenerate length of the *Tg*(*NTR*) fish treated with 15 mM MTZ. For this reason, the following comparisons will focus on 5 and 10 mM treated *Tg*(*NTR*) fish.

Beginning with comparing the first three segment lengths of 5 and 10 mM MTZ treated *Tg*(*NTR*) fish to the WT MTZ fish treated with the same MTZ concentration, it was found that in each case the *Tg*(*NTR*) fish had significantly shorter bone segments (Fig. 3.2.2 A-C). This indicated based on previous conclusions that joint cells were being ablated, causing the shortened segments. Comparing the lengths of the same three segments between 5 and 10 mM MTZ-treated *Tg*(*NTR*) fish there was a significant decrease in the length of the segment of 10 mM MTZ-treated *Tg*(*NTR*) fish compared to those treated with 5 mM. This agreed with our previous conclusion that the segment length reduction is tied to the lifting of inhibition of joint formation. In this case we must assume that 5 mM MTZ treatments ablate some cells, but not as many as 10 mM MTZ treatment. This would allow the *hoxa13a* threshold to be reached earlier than the control fish, but later than 10 mM MTZ-treated *Tg*(*NTR*) fish.

The results of the concentration gradient also fit with the proposed model for the formation of the first joint. When comparing the distance from the wound to the first formed joint in 5 and 10 mM MTZ-treated *Tg*(*NTR*) fish to the WT fish treated with MTZ of the same concentration there was a significant difference in distance in both cases (Fig.

3.2.3). When distance of the first joint was compared between the 5 and 10 mM MTZ-treated *Tg*(*NTR*) fish, a significant difference between the two was observed. Following the same reasoning as above, the 5 mM MTZ treatment must have reduced proliferation in the blastema to a greater extent than in the 10 mM treatment.

4.4 Similar models involving hox gradients

In the failure to eliminate joints during regeneration we have indirectly provided support for a proposed model of joint formation during regeneration. From the data we have gathered we concluded that the phenotypes observed were due in part to changes in *hoxa13a* expression creating a gradient. Although this proposed model and these results that support it are in the early stages of development, it is believed that the formation of gradients contribute to limb patterning (Weiss, 1947). Gradient models of *hox* genes involved in a variety of structure formation across multiple species including development of the chicken wing bud as well as the limb bud of *xenopus* and mouse embryos (Chuong et al., 1990; Oliver et al., 1989). In zebrafish gradients of *hoxa1a*, a homologue to *XIHbox1*, the first vertebrate homeobox gene discovered in *Xenopus* (Oliver et al., 1989), were found throughout the development of the embryo. *hoxa1a* is first detected in somites at 14 hpf and in the pectoral fin bud at 19 hpf, and a gradient is noticeable by 48 hpf. The *hox* gradient pattern observed in zebrafish embryos during development resembled *hox* gradients observed in early development of frogs and mice (Molven, Wright, Bremiller, De Robertis, & Kimmel, 1990).

4.5 Alternative methods for targeted joint cell ablation during regeneration

A very likely reason why joint cells were not completely ablated during regeneration is related to the lack of efficiency of the NTR/MTZ system. In the transgene

used to make the NTR fish, YFP was inserted upstream of NTR cDNA making it difficult to tell how much NTR was being translated although in theory there should be equimolar concentrations. The *Inta11 intron* enhancer that was used may not have been an optimal enhancer as it is driving expression in a few cells of the blastema (albeit at low level) during regeneration which has already been stated as a serious concern in the phenotypes we observed. To remedy the problems of this line there are a couple solutions.

The first solution would be to determine regulatory elements which drive expression solely in the presumptive and maturing joint cells. Ideal candidates include *evx1* and *pthrp1*. Our lab has attempted to determine the regulatory elements for *evx1*, but so far has not been successful.

The second option uses *Inta11* regulatory elements which are currently the best option available to target developing joint cells and a more recent ablation technique called Apoptosis Through Targeted Activation of Caspase 8. This technique uses a caspase 8-FKBP fusion protein whose expression is driven by a tissue-specific promoter and in the presence of AP20187, an analogue of FK506, two FKBP domains are brought into close proximity, which in turn causes the fusion protein containing caspase 8 to dimerize activating a signal cascade leading to apoptosis (Clackson et al., 1998; Trujillo, Pajvani, & Scherer, 2005). This technique has been utilized effectively in mice to ablate adipose cells with an efficiency of over 95% (Trujillo et al., 2005). More recently this method has been adapted to zebrafish and involved replacing the FKBP with a mutated tamoxifen-interacting estrogen receptor ligand-binding domain (ER^{T2}) which in the presence of tamoxifen cause caspase 8 to dimerize and initiate the apoptotic cascade similar to the technique used in mice (Chu, Senghaas, Köster, Wurst, & Kühn, 2008; Weber et al., 2016).

This approach will present the same limitations as the NTR/MTZ (potential death of the blastemal and actinotrichia-forming since the same Inta11 regulatory element would be used) however, it is possible that cell ablation may be more efficient than with the NTR/MTZ system.

4.6 Ectopic expression of cell fate commitment markers during regeneration

During regeneration of the caudal fin the *runx2a/b*-expressing cells have been shown to initiate the osteoblast commitment cascade followed by the expression of *sp7*. We believe that the *runx2a/b*-expressing cells can commit to a second fate which is joint cell formation potentially induced by the expression of *hoxa13a*. To determine if *runx2a*-expressing cells are responsible for joint cell formation, we chose to create transgenic fish lines in order to i) ectopically express the bone commitment marker *sp7* in the cells to see if joints fail to form and ii) ectopically express *hoxa13a* in the *runx2a*-expressing cells to determine if this will inhibit osteoblast formation. These lines will use the LoxP/Cre inducible recombination system to control the expression of commitment markers giving the ability to conditionally control the fate of the uncommitted *runx2a/b* positive distal cells.

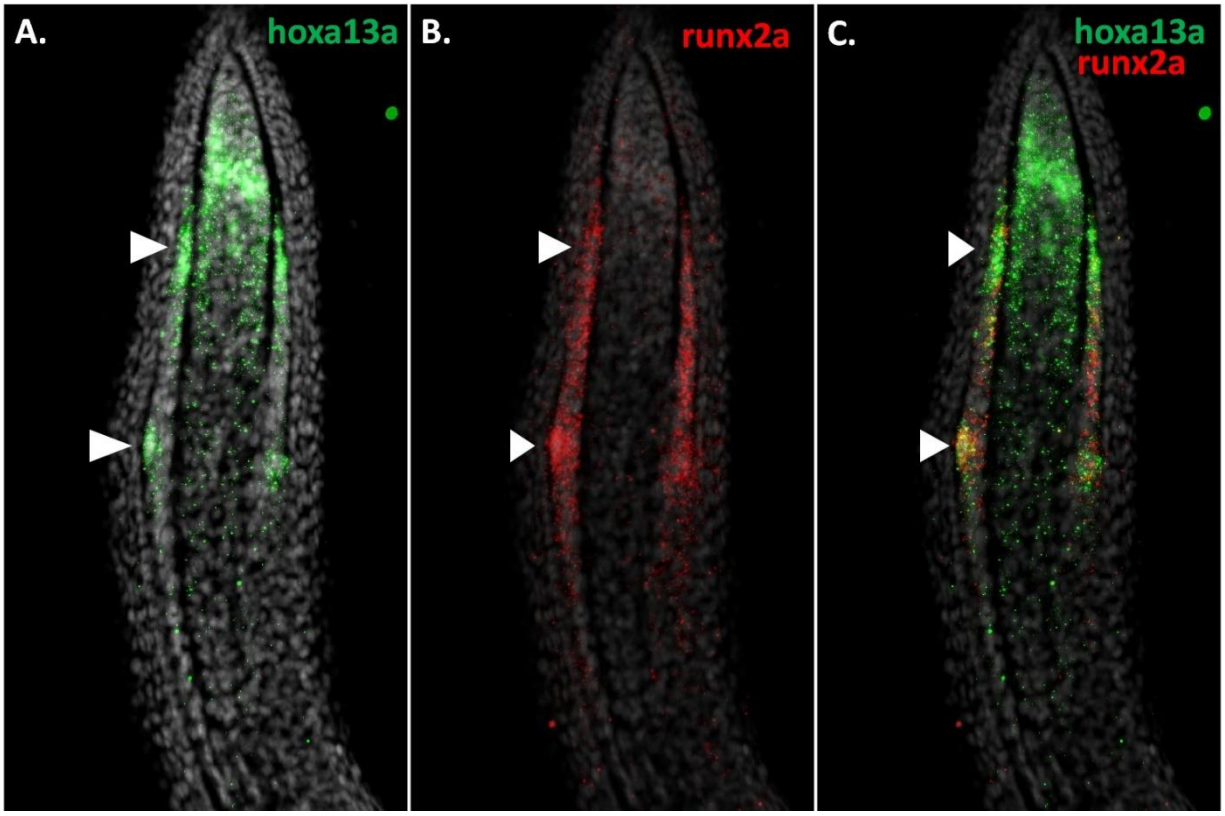

Figure 4.6.1 Overlapping expression of *runx2a* and *hoxa13a* in the regenerating fin ray.
Expression pattern of *hoxa13a* (**A**) compared to *runx2a* (**B**) along with merged image (**C**) showing expression in presumptive and committed joint regions. Photos taken by J. Zhang.

4.6.1 Ectopic expression of *sp7* during regeneration

In order to ectopically express *sp7*, the bone cell commitment marker, in the presumptive joint cells during regeneration the constructs *Tg(Inta11-β-globin:Loxp mcherry Loxp-sp7-2A-eGFP)* and *Tg(runx2a-β-globin:* ^{ERt2}Cre^{ERt2}*-2A-mcherry)* were created. The *Inta11 intron* regulatory elements along with a β-globin minimal promoter drives expression in the pre-osteoblasts and committed joints during regeneration (Figure 4.6.1A). This will drive the expression of mCherry flanked by Loxp sites. After the stop which is between mCherry cDNA and Loxp is sp7 cDNA, 2A, and eGFP cDNA. (Sp7, 2A, eGFP*)* will be transcribed as one long piece of mRNA and during translation the 2A peptide

self cleaves leaving equimolar concentrations of *sp7* and eGFP. In the second construct, the *runx2a* regulatory elements along with a β-globin minimal promoter give expression in the pre and mature osteoblasts, also including the area where joints commit and maturing joints (Figure 4.6.1B). This will drive expression of Cre fused to two mutated estrogen receptors ($^{ERt2}Cre^{ERt2}$) followed by 2A and mCherry. After a stable line of transgenic fish is established for each construct, the lines will be crossed to create double transgenic fish. Once the double transgenic is created the overlap of expression will occur in the joint committing region of *runx2a* and the developing joint (Figure 4.6.1C).

During the proposed experiments the caudal fin of double transgenic fish will be amputated in standard fashion. In the absence of tamoxifen the $^{ERt2}Cre^{ERt2}$ will only be present in the cytoplasm (Figure 4.6.2). Once tamoxifen is present it will bind to the mutated estrogen receptor allowing it to translocate into the nucleus along with *Cre.* In the nucleus, Cre will recognize the *loxp* sites and excise the *loxP- mcherry-loxP* sequence (Figure 4.6.2). This will allow for the expression of *sp7* in the presumptive joints which in turn should result in presumptive joint cells becoming osteoblasts and the fin regenerate should form with an absence of joints. This will also cause a change in fluorescence in these cells from only expressing mCherry and appearing red, to expressing both mCherry and eGFP appearing yellow under a merged image. Currently this construct is being microinjected into single cell embryos and the primary injected fish are being grown up. These fish will be screened for mCherry expression and positive founder fish will be used to create the double transgenic fish.

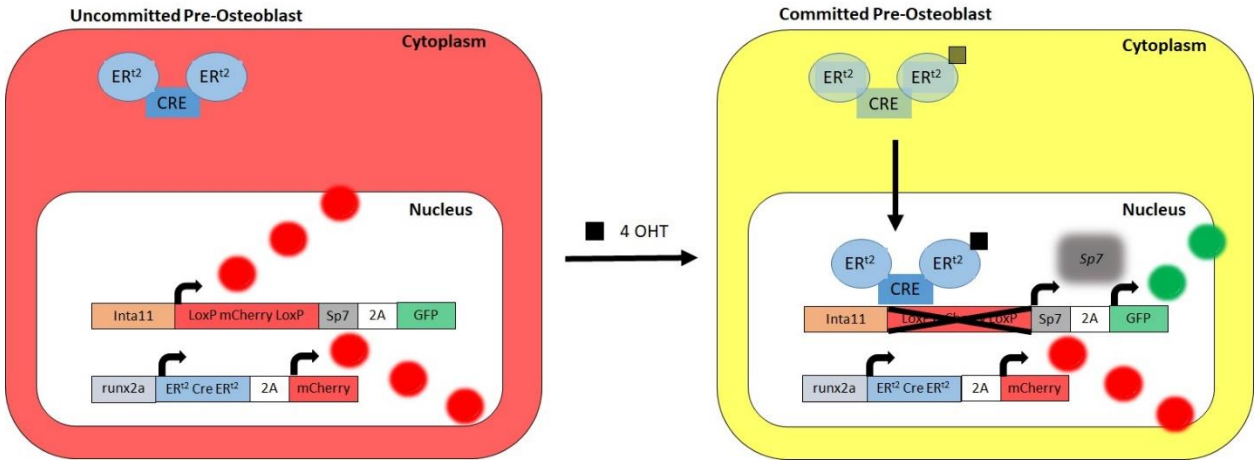

Figure 4.6.2 Tamoxifen allows ectopic expression of s*p7* in double transgenic line.
The uncommitted joint cells will appear red under UV through the double expression of mCherry. In the presence of tamoxifen (4-OHT) which will bind to the mutated estrogen receptor (ERt2) translocated it along with Cre into the nucleus where it excises the mCherry loxP. This will lead the cells to express both eGFP and mCherry allowing for confirmation of *sp7* expression.

4.6.2 Ectopic expression of *hoxa13a* during regeneration

In similar fashion as described above we wanted to express *hoxa13a* in the *runx2a/b* expressing cells to see if we could entice them to solely commit to becoming joint cells. This would very strongly support our belief that *runxa/b* expressing cells not only have two fates, but that *hoxa13a* can direct this group of cells to become joint cells and acts upstream or in parallel of *evx1*. Once again the *Tg(runx2a-β globin:* $^{ERt2}Cre^{ERt2}$*-2A-mcherry)* described above will be the line used to provide the $^{ERt2}Cre^{ERt2}$ required to cut at Loxp sites. The second construct created was *Tg(runx2a-β globin:Loxp mcherry Loxp-hoxa13a-2A-eGFP)* using the same *runx2a* regulatory element to give overlap of expression in the joint and osteoblast forming area. We wanted a complete overlap in expression in this case because we want all *runx2a* positive cells to ectopically express *hoxa13a*, hopefully committing them all to joint cell lineage potentially leading to a regenerate that lacks osteoblasts.

To control this inducible ectopic expression, the *runx2a* regulatory elements along with a β-globin minimal promoter will drive expression of *Loxp mcherry Loxp*. Once this sequence is removed by *Cre*, *hoxa13a*, 2A, and eGFP will be transcribed as one long mRNA and upon translation will give equimolar concentrations of *hoxa13a* and eGFP.

In an identical manner to the ectopic expression of *sp7*, in the absence of tamoxifen the uncommitted pre-osteoblasts will appear red under UV through expression of mCherry and $^{ERt2}Cre^{ERt2}$ will be found only in the cytoplasm (Figure 4.6.3). When tamoxifen is present it will bind to $^{ERt2}Cre^{ERt2}$ allowing the complex to enter the nucleus and remove the Loxp mCherry Loxp, resulting in the expression of both *hoxa13a* and eGFP. This will cause the cells to appear yellow in a merge image due to the presence of eGFP and mCherry, also allowing the confirmation that *hoxa13a* is being translated. Currently this construct is being microinjected into single cell embryos and the primary injected fish are being grown up. These fish will be screened for mCherry expression and positive founder fish will be used to create the double transgenic fish.

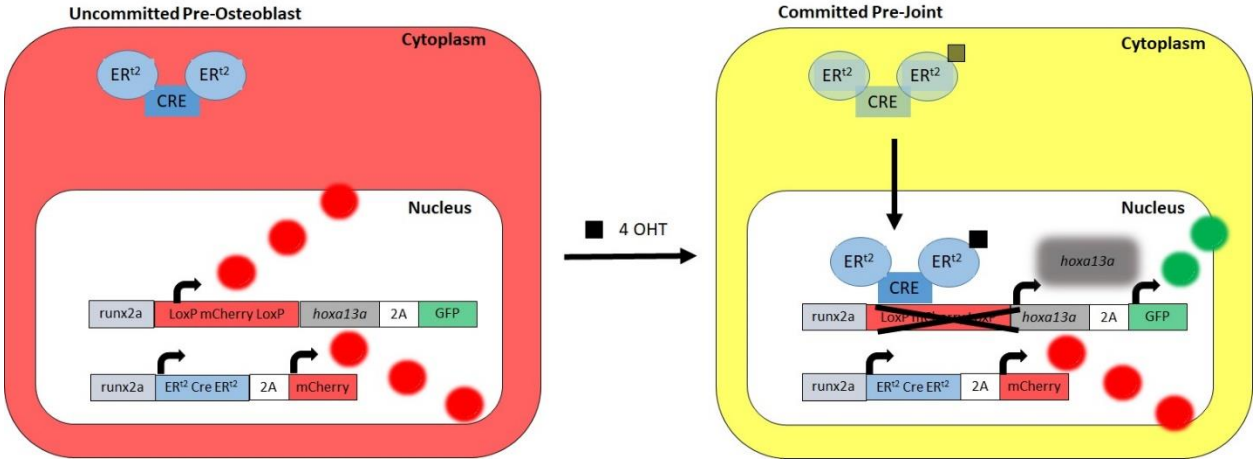

Figure 4.6.3 Tamoxifen allows for ectopic expression of *hoxa13a* in the double transgenic line.

The uncommitted joint cells will appear red under UV through the double expression of mCherry. In the presence of tamoxifen (4-OHT) which will bind to the mutated estrogen receptor (ERt2) translocated it along with Cre into the nucleus where it excises the mCherry loxP. This will lead the cells to express both eGFP and mCherry allowing for confirmation of *hoxa13a* expression.

4.7 Ectopic expression of cell fate commitment factors in pre-osteoblasts

In the second objective, the goal was to ectopically express the osteoblast commitment factor *sp7* and the hypothesized joint commitment factor *hoxa13a* in the presumptive joint cells to determine if they would commit to bone and joint cells respectively. It has been shown that *sp7* is an osteoblast intermediate commitment factor in the *runx2a*-expressing pre-osteoblasts (Knopf et al., 2011). We also believe that *hoxa13a* may be a commitment factor for joint cells from the same group of *runx2a*-expressing cells because its expression precedes *evx1* in the presumptive joint cells. During the regenerative process by controlling which of the two intermediate commitment factors are expressed in the pre-osteoblast cells we should be able to control their fate as they mature.

4.7.1 Preliminary results for of ectopic expression of *sp7* during regeneration

This portion of the project is in the early stages of establishing the transgenic lines of *Tg(Inta11-β-globin:Loxp mcherry Loxp-sp7-2A-eGFP)* and *Tg(runx2a-β-globin:* ^{ERt2}Cre^{ERt2}*-2A-mcherry).* The expected outcome of double transgenic fish following treatment with tamoxifen should be a regenerating fin that lacks joints. The *inta11* and *runx2a* enhancers have an overlap of activated expression with the pre-osteoblast cells, specifically when the presumptive joint cells cluster (Figure 4.6.1). During regeneration the expression of *sp7* will be induced with tamoxifen treatment, which will allow the Cre recombinase to enter the nucleus of the pre-osteoblast cells, excise the loxP-mCherry-loxP sequence and allow for the transcription and translation of *sp7* and eGFP. Based on previous studies we hypothesize that the presence of *sp7* early in joint cell commitment (even in the presence of high level of *hoxa13a* expression) will override it and change fate to become an osteoblast.

Although currently no work has been done on fate switching in presumptive joint cells during regeneration, previous studies have examined bone regeneration through dedifferentiation of osteoblasts during regeneration. These studies have shown that in the area proximal to the wound at 2 dpa there is an upregulation of *runx2a*, indicating that the osteoblasts are dedifferentiating, and this increased expression of *runx2a* also covers joints immediately proximal to the wound (Knopf et al., 2011). When osteoblasts are nearly completely ablated prior to amputation in the caudal fin, regeneration occurs in the fin rays at nearly the same rate as controls indicating that there are other cell types which can replace the lost osteoblast and form bone during this process (Singh et al., 2012). It would make sense that the other cells dedifferentiating and regenerating the osteoblasts are the cells with which they share a common cell lineage with, which we believe are the joint

forming cells. Since the osteoblasts have a restricted cell lineage and can only form other osteoblasts, we believe that *sp7* expression in the presumptive joint cells will lead to the formation of a regenerate that lacks joints completely.

There exists potential pitfalls that may hamper the expected outcome of this experiment. The efficiency with which Cre is expressed and the efficiency of the Cre recombinase activity will have a direct outcome on how well the cells are directed into becoming osteoblasts. Another factor that will influence the results will be the levels of *sp7* required to override the cells that are being committed to becoming joints. This will depend on how strongly the enhancers in the double transgenic fish express *sp7* and Cre. Finally, the penetrative ability and binding efficiency of tamoxifen to the ERt2 binding domain will affect how much Cre can be translocated into the nucleus will also be a factor in how successful this experiment will be. However, this is of least concern as the CreERt2 system has be used successfully in zebrafish numerous times.

4.7.2 Preliminary results for of ectopic expression of *hoxa13a* during regeneration

Similar to the ectopic expression of *sp7* during regeneration mentioned above, this portion of the project is still in early stages of creating the transgenic lines. This project will ectopically express *hoxa13a*, which we hypothesize to be a joint commitment factor. A double transgenic line created from the following two transgenic lines will be used to accomplish this; *Tg(runx2a-β-globin:* ^{ERt2}Cre^{ERt2}*-2A-mcherry)* and *Tg(runx2a-β globin:Loxp-mcherry-Loxp-hoxa13a-2-eGFP)*. In this case we are using the same promoter in both constructs because we want all of the *runx2a* expressing cells to become joint cells. If during regeneration we do not see the formation of bone, then further evidence that joint and bone cells share a common lineage will be provided. There is still much to be learned

about joint cell regeneration in the caudal fin of zebrafish and the involvement of *hoxa13a* in this process is novel, making predictions of the outcome relatively difficult. Studies in the ablation of osteoblasts during fin regeneration in zebrafish have shown that through mass ablation of osteoblasts using the MTZ/NTR system, fins will still regenerate relatively normally once treatment is stopped (Singh et al., 2012). This would suggest that for our double transgenic line to produce a boneless fin regenerate there would need to be a presence of tamoxifen to continually drive high enough expression of *hoxa13a* to reach the threshold in the pre-osteoblasts and that once this has been halted, bone may begin to form once more. Studies have also shown that by indirectly inhibiting the formation of the *runx2a*-expressing cells, the entire process of regeneration is halted (Stewart et al., 2014), and that in zebrafish with early stage joint marker *evx1* knocked out fins form with only bones (Ton & Iovine, 2013). It is unknown however what will occur when the osteoblast commitment pathway is blocked and *runx2a* expressing cells become solely joint cells. Even if we cannot get a complete absence of bone, this experiment should allow us to determine if *hoxa13a* is acting upstream of *evx1*as opposed to in parallel. If we observe activation of *evx1* expression in cells that express high levels of *hoxa13a*, this would show that *hoxa13a* results in the activation of *evx1*.

Similar to the ectopic expression of *sp7* there exists almost identical potential pitfalls that may affect the expected outcome of this experiment. The efficiency with which Cre is expressed and the efficiency of the Cre recombinase activity will have a direct outcome on how well the cells are directed into becoming osteoblasts. If *sp7* does have the ability to override *hoxa13a* in the previous experiment, then ectopic expression of *hoxa13a* will have to begin before the onset of *sp7*expression. This will be required in order to

commit the *runx2a*-expressing cells into joint cells before they are committed to becoming osteoblasts. The other potential pitfalls of this experiment are identical to those seen in the ectopic expression of *sp7* as the same technique is been used to induce the expression.

4.8 Assessing joint quality

A test to assess joint quality is something that should be used in future experiments. Since there is much to be learned about the fibrous joints of the fin in zebrafish, the assessment will have to be based on what can be directly observed using what is known now. In wild type fish imaged under a bright field filter, a healthy joint appears as a white line across the fin ray. These lines are almost perfectly straight across. The first step of the test should be to classify the joints as good quality (the white line goes across the whole ray), intermediate quality (the white line goes between 50-99% across the fin ray), poor quality (white line goes <50% of the way across), and indeterminable (joint is up such poor quality no joint can be measured). In most cases the white line may only go a portion of the way across the ray but the joint is still measurable all the way across as a thin line can still be seen. For the second step of the test the joint length should be measured and compared to the thickness of the fin ray measured at a decided unit proximal and distal to the joint as well as through the center of the joint. The length of the joint should be taken as a ratio over the averaged bone width. Scores that are close to 1 mean that the joint is perpendicular to the fin ray indicating optimal formation. In fish treated with MTZ where the joints are often angled or ‘U’ shaped, these joint lengths will be longer and will produce a ratio greater than 1.

5 Conclusion

The fish of infraclass teleost retain the ability to regenerate organs and appendages once damaged to their original size and shape, a function that has been generally lost in higher vertebrates. Teleost include zebrafish which have become a model organism for studying regeneration, and the caudal fin in particular has become the focus of regenerative studies of dermal bone because of the relatively simple tissue makeup. The fin rays (lepidotrichia) are the bony structures found in the caudal fin and consist of segmented bone separated by fibrous joints. How these joints develop and regenerate is an area that has not been well studied and much remains unknown. It has been suggested that the bone cells (osteoblasts) and joint cells share a common lineage but differentiate into their fates based on expression of specific commitment pathways. This led us to ask the question: what happens if we completely ablate joint cells during regeneration? In order to accomplish this, we set up three objectives: **1**. Eliminate joint cells in the regenerating caudal fin using the metronidazole(MTZ)/nitroreductase(NTR) inducible genetic ablation technique. **2**. Ectopically express the bone commitment marker *sp7* in the common lineage cells during regeneration to drive all cells to become bone. **3**. Ectopically express hypothesized joint commitment factor *hoxa13a* in common lineage cells to drive cells to become joints.

1. To target joint cells for ablation we used a transgenic line of zebrafish previously created in our lab was used, Tg(I*nta11-β-globin:YFP-2A-NTR*). Surprisingly however, when these fish were treated with 10 mM of MTZ the joints still formed. However, fin rays show reduced length of bone segments and reduced joint quality as judged by the quality of the white joint line. This suggested that joint cells were being ablated but it was only a partial ablation, which agreed with our proposed joint formation model.

2. In the ectopic expression of the bone commitment marker *sp7* involved creating two constructs: *Tg(Inta11-β-globin:Loxp mcherry Loxp-sp7-2A-eGFP)* and *Tg(runx2a-β-globin:* ^{ERt2}Cre^{ERt2}*-2A-mcherry)*. We expect that once the double transgenic fish is created, we will be able to induce the formation of a regenerating fin that lacks joints.

3. In the ectopic expression of the hypothesized joint cell commitment marker *hoxa13a* a third construct was created: *Tg(runx2a-β globin:Loxp mcherry Loxp-hoxa13a-2A-eGFP)* which will be used with the previously mentioned construct *Tg(runx2a-β-globin:* ^{ERt2}Cre^{ERt2}*-2A-mcherry)* to create a double transgenic line. By using the same enhancer that is found in all the common lineage cells of osteoblasts and joint cells we hope to convert all the cells to become joint cells, resulting in a regenerate that lacks bone.

Understanding where joint cells are derived from in zebrafish during caudal fin regeneration would add an important part to the puzzle of completely understanding regeneration. Until we better understand the process as a whole it will be difficult to relate it to helping humans. The dermal bone found in the fin rays is the same type of bone found in the skull of humans (Laue et al., 2011), and understanding how it regenerates in organisms that still possess the ability naturally could lead to medical breakthroughs in fixing damage to these bones in humans. The same can be said for the fibrous joints in the caudal fin. There are many degenerative joint problems in humans and if we determine how joints regenerate then this may lead to treatment for people who suffer from these problems.

6 Appendix

6.1 Molecular cloning

6.1.1 *Tg* (*Inta11-β globin:Loxp mcherry Loxp-sp7-2A-eGFP*)

To create the construct (*Int11-β globin:Loxp mcherry Loxp-sp7-2A-eGFP*) *Inta11-β globin*, *Loxp mcherry Loxp*, and *sp7* were first cloned individually into *pDrive* cloning vectors (Qiagen). *Inta11-β globin* was then sub-cloned into (Tol2:2A-eGFP Tol2) between the upstream Tol2 arm and 2A. This was followed by sub-cloning *sp7* between *Inta11-β globin* and 2A. Finally *Loxp mcherry Loxp* was sub-cloned into the construct between *Inta11-β globin* and *sp7*.

6.1.2 *Tg* (*runx2a-β globin:^{Ert2}Cre^{Ert2}-2A-mcherry*)

To create the construct (*runx2a:β globin:^{Ert2}Cre^{Ert2}-2-mcherry*) the human *runx2a* enhancer was amplified from DNA in accordance with Knopf et al (2011) and cloned into a *pDrive* cloning vector (Qiagen). *β globin* and ^{Ert2}*Cre*^{Ert2} were also cloned into a *pDrive* cloning vector (Qiagen). The human *RUNX2A* was then sub-cloned into (Tol2:2A eGFP Tol2) between the upstream Tol2 arm and 2A. This was followed by *β globin* between *runx2a* and 2A and finally ^{Ert2}*Cre*^{Ert2} between *β globin* and 2A.

2A was cloned into *pDrive* and screen for forward orientation in the SP6 promoter direction. The 2A *pDrive* vector was then linearized with *BamHI* and *KpnI* digestion site and *mcherry* was sub-cloned in. 2A-*mcherry* was then digested out as a single piece. 2A-eGFP in the aforementioned construct containing *runx2a* was digested out with the same sites as 2A-*mcherry* and subsequently replaced by it to finalize the construct.

6.1.3 *Tg* (*runx2a-β globin:Loxp mcherry Loxp-hoxa13a-2A-eGFP*)

To create the construct (*runx2a-β globin:Loxp mcherry Loxp-hoxa13a-2A-eGFP*) the template of partially finished (*runx2a-β globin:*^{Ert2}*Cre*^{Ert2}*-2A-mcherry*) was used when it was at the (*runx2a-β globin:2A*-eGFP) stage. *Loxp mcherry Loxp* and *hoxa13a* were cloned into individually into *pDrive* cloning vectors (Qiagen). First *hoxa13a* was sub-cloned into (*runx2a-β globin:2A*-eGFP) between *β globin* and 2A. *Loxp mcherry Loxp* was sub-cloned in between *β globin* and *hoxa13a* to complete the construct.

6.2 Microinjection of zebrafish embryos

Zebrafish breeding traps were set up as described above the night before and the following morning were allowed to breed for 15 minutes to ensure embryos collected were at the single cell stage. Embryos were placed on a 2% agarose gel plate that contained triangular indented rows that held the embryos in place during injection. The needles used were borosilicate glass tubes with an inner diameter of 0.5mm, an outer diameter of 1.0 mm and 10 cm long (Sutter Instruments). These tubes were pulled into thinner diameter using a Sutter instruments Flaming/Brown P-87 model micropipette puller. Before use the needles were cut with a scalpel blade to create an appropriately sized tip for injection. The needle was then filled 1 µl of injection solution from 2 µl of a combination of stock injection solution (100 nl/µl construct, 200 mM KCl, 0.05% phenol red) and transpose RNA (50 ng/µl). Embryos were injected and left in UV treated water overnight and bleached the following morning.

6.3 Screening for transgenic fish lines

Once fish had been injected with a construct they were left in E3 media for 24 hours. At that time, they were screen for the presence of GFP or mCherry. This began with

dechorination of the embryos using forceps and anesthetizing fish in 0.1mg/ml tricaine in E3 media. GFP/mCherry positive fish were collected and sent to be raised to adulthood in a designated growing room.

7 References

Abzhanov, A., Rodda, S. J., McMahon, A. P., & Tabin, C. J. (2007). Regulation of skeletogenic differentiation in cranial dermal bone. *Development (Cambridge, England)*, *134*(17), 3133–3144. https://doi.org/10.1242/dev.002709

Akimenko, M. A., Marí-Beffa, M., Becerra, J., & Géraudie, J. (2003). Old questions, new tools, and some answers to the mystery of fin regeneration. *Developmental Dynamics*, *226*(2), 190–201. https://doi.org/10.1002/dvdy.10248

Ariga, J., Walker, S. L., & Mumm, J. S. (2010). Multicolor time-lapse imaging of transgenic zebrafish: visualizing retinal stem cells activated by targeted neuronal cell ablation. *Journal of Visualized Experiments : JoVE*, (43), 2–7. https://doi.org/10.3791/2093

Askary, A., Smeeton, J., Paul, S., Schindler, S., Braasch, I., Ellis, N. A., … Gage Crump, J. (2016). Ancient origin of lubricated joints in bony vertebrates. *eLife*, *5*(2016JULY). https://doi.org/10.7554/eLife.16415

Bakkers, J. (2011). Zebrafish as a model to study cardiac development and human cardiac disease. *Cardiovascular Research*. https://doi.org/10.1093/cvr/cvr098

Borday, V., Tharon, C., Avaron, F., Brulfert, A., Casane, D., Laurenti, P., & Graudie, J. (2001). evx1 Transcription in bony fin rays segment boundaries leads to a reiterated pattern during zebrafish fin development and regeneration. *Developmental Dynamics*, *220*(2), 91–98.

https://doi.org/10.1002/1097-0177(2000)9999:9999<::AID-DVDY1091>3.0.CO;2-J

Canadian Council on Animal Care. (2005). Canadian Council on Animal Care guidelines on: the care and use of fish in research, teaching and testing. *Canadian Council on Animal Care*, 1–94. Retrieved from http://www.ccac.ca/Documents/Standards/Guidelines/Fish.pdf

Cardeira, J., Gavaia, P. J., Fernández, I., Cengiz, I. F., Moreira-Silva, J., Oliveira, J. M., … Laizé, V. (2016). Quantitative assessment of the regenerative and mineralogenic performances of the zebrafish caudal fin. *Scientific Reports*, *6*, 39191. https://doi.org/10.1038/srep39191

Chen, C. F., Chu, C. Y., Chen, T. H., Lee, S. J., Shen, C. N., & Hsiao, C. Der. (2011). Establishment of a transgenic zebrafish line for superficial skin ablation and functional validation of apoptosis modulators in vivo. *PLoS ONE*, *6*(5). https://doi.org/10.1371/journal.pone.0020654

Chitnis, A. B., Dalle Nogare, D., & Matsuda, M. (2012). Building the posterior lateral line system in zebrafish. *Developmental Neurobiology*, *72*(3), 234–255. https://doi.org/10.1002/dneu.20962

Chu, Y., Senghaas, N., Köster, R. W., Wurst, W., & Kühn, R. (2008). Novel Caspase-suicide proteins for tamoxifen-inducible apoptosis. *Genesis*, *46*(10), 530–536. https://doi.org/10.1002/dvg.20426

Chuong, C.-M., Oliver, G., Ting, S. a, Jegalian, B. G., Chen, H. M., & De Robertis, E. M. (1990). Gradients of homeoproteins in developing feather buds. *Development (Cambridge, England)*, *110*(1990), 1021–1030.

Clackson, T., Yang, W., Rozamus, L. W., Hatada, M., Amara, J. F., Rollins, C. T., … Holt, D. A.

(1998). Redesigning an FKBP-ligand interface to generate chemical dimerizers with novel specificity. *Proceedings of the National Academy of Sciences of the United States of America*, *95*(18), 10437–42. https://doi.org/10.1073/pnas.95.18.10437

Cox, J. A., Zhang, B., Pope, H. M., & Voigt, M. M. (2016). Transcriptome analysis of chemically-induced sensory neuron ablation in zebrafish. *PLoS ONE*, *11*(2). https://doi.org/10.1371/journal.pone.0148726

Curado, S., Anderson, R. M., Jungblut, B., Mumm, J., Schroeter, E., & Stainier, D. Y. R. (2007). Conditional targeted cell ablation in zebrafish: A new tool for regeneration studies. *Developmental Dynamics*, *236*(4), 1025–1035. https://doi.org/10.1002/dvdy.21100

Curado, S., Stainier, D. Y. R., & Anderson, R. M. (2008). Nitroreductase-mediated cell/tissue ablation in zebrafish: a spatially and temporally controlled ablation method with applications in developmental and regeneration studies. *Nature Protocols*, *3*(6), 948–954. https://doi.org/10.1038/nprot.2008.58

Dardis G, Tryon R, Ton Q, Johnson SL, I. M. (2017). Cx43 suppresses evx1 expression to regulate joint initiation in the regenerating fin. *Developmental Dynamics, Epub ahead*. https://doi.org/10.1002

Durán, I., Marí-Beffa, M., Santamaría, J. A., Becerra, J., & Santos-Ruiz, L. (2011). Actinotrichia collagens and their role in fin formation. *Developmental Biology*, *354*(1), 160–172. https://doi.org/10.1016/j.ydbio.2011.03.014

Eames, B. F., Amores, A., Yan, Y.-L., & Postlethwait, J. H. (2012). Evolution of the osteoblast: skeletogenesis in gar and zebrafish. *BMC Evolutionary Biology*, *12*(1), 27. https://doi.org/10.1186/1471-2148-12-27

Gavaia, P. J., Simes, D. C., Ortiz-Delgado, J. B., Viegas, C. S. B., Pinto, J. P., Kelsh, R. N., … Cancela, M. L. (2006). Osteocalcin and matrix Gla protein in zebrafish (Danio rerio) and Senegal sole (Solea senegalensis): Comparative gene and protein expression during larval development through adulthood. *Gene Expression Patterns*, *6*(6), 637–652. https://doi.org/10.1016/j.modgep.2005.11.010

Gemberling, M., Bailey, T. J., Hyde, D. R., & Poss, K. D. (2013). The zebrafish as a model for complex tissue regeneration. *Trends in Genetics*. https://doi.org/10.1016/j.tig.2013.07.003

Goldsmith, M. I., Iovine, M. K., O'Reilly-Pol, T., & Johnson, S. L. (2006). A developmental transition in growth control during zebrafish caudal fin development. *Developmental Biology*, *296*(2), 450–457. https://doi.org/10.1016/j.ydbio.2006.06.010

Gray, C., Loynes, C. A., Whyte, M. K. B., Crossman, D. C., Renshaw, S. A., & Chico, T. J. A. (2011). Simultaneous intravital imaging of macrophage and neutrophil behaviour during inflammation using a novel transgenic zebrafish. *Thrombosis and Haemostasis*, *105*(5), 811–819. https://doi.org/10.1160/TH10-08-0525

Grotek, B., Wehner, D., & Weidinger, G. (2013). Notch signaling coordinates cellular proliferation with differentiation during zebrafish fin regeneration. *Development (Cambridge, England)*, *140*(7), 1412–23. https://doi.org/10.1242/dev.087452

Haffter, P., Odenthal, J., Mullins, M. C., Lin, S., Farrell, M. J., Vogelsang, E., … Nüsslein-Volhard, C. (1996). Mutations affecting pigmentation and shape of the adult zebrafish. *Development Genes and Evolution*, *206*(4), 260–276. https://doi.org/10.1007/s004270050051

Hans, S., Kaslin, J., Freudenreich, D., & Brand, M. (2009). Temporally-controlled site-specific

recombination in zebrafish. *PLoS ONE*, *4*(2). https://doi.org/10.1371/journal.pone.0004640

Hayes, A. J., Reynolds, S., Nowell, M. A., Meakin, L. B., Habicher, J., Ledin, J., … Hammond, C. L. (2013). Spinal Deformity in Aged Zebrafish Is Accompanied by Degenerative Changes to Their Vertebrae that Resemble Osteoarthritis. *PLoS ONE*, *8*(9). https://doi.org/10.1371/journal.pone.0075787

Hoess, R. H., Wierzbicki, A., & Abremski, K. (1986). The role of the loxP spacer region in P1 site-specific recombination. *Nucleic Acids Research*, *14*(5), 2287–300. https://doi.org/10.1093/nar/gkn942

Hoptak-Solga, A. D., Nielsen, S., Jain, I., Thummel, R., Hyde, D. R., & Iovine, M. K. (2008). Connexin43 (GJA1) is required in the population of dividing cells during fin regeneration. *Developmental Biology*, *317*(2), 541–548. https://doi.org/10.1016/j.ydbio.2008.02.051

Hsu, C. C., Hou, M. F., Hong, J. R., Wu, J. L., & Her, G. M. (2010). Inducible male infertility by targeted cell ablation in zebrafish testis. *Marine Biotechnology*, *12*(4), 466–478. https://doi.org/10.1007/s10126-009-9248-4

Hunziker, E. B. (1994). Mechanism of longitudinal bone growth and its regulation by growth plate chondrocytes. *Microsc Res Tech*, *28*(6), 505–519. https://doi.org/10.1002/jemt.1070280606

Iovine, M. K., Higgins, E. P., Hindes, A., Coblitz, B., & Johnson, S. L. (2005). Mutations in connexin43 (GJA1) perturb bone growth in zebrafish fins. *Developmental Biology*, *278*(1), 208–219. https://doi.org/10.1016/j.ydbio.2004.11.005

Iovine, M. K., & Johnson, S. L. (2000). Genetic analysis of isometric growth control mechanisms in the zebrafish caudal fin. *Genetics*, *155*(3), 1321–1329.

Kague, E., Roy, P., Asselin, G., Hu, G., Simonet, J., Stanley, A., … Fisher, S. (2016). Osterix/Sp7 limits cranial bone initiation sites and is required for formation of sutures. *Developmental Biology, 413*(2), 160–172. https://doi.org/10.1016/j.ydbio.2016.03.011

Kawakami, A. (2010). Stem cell system in tissue regeneration in fish. *Development, Growth & Differentiation*, *52*, 77–87. https://doi.org/10.1111/j.1440-169X.2009.01138.x

Kherdjemil, Y., Lalonde, R. L., Sheth, R., Dumouchel, A., de Martino, G., Pineault, K. M., … Kmita, M. (2016). Evolution of Hoxa11 regulation in vertebrates is linked to the pentadactyl state. *Nature*, *539*(7627), 89–92. https://doi.org/10.1038/nature19813

Knopf, F., Hammond, C., Chekuru, A., Kurth, T., Hans, S., Weber, C. W., … Weidinger, G. (2011). Bone regenerates via dedifferentiation of osteoblasts in the zebrafish fin. *Developmental Cell*, *20*(5), 713–724. https://doi.org/10.1016/j.devcel.2011.04.014

Knox, R. J., Friedlos, F., Jarman, M., & Roberts, J. J. (1988). A new cytotoxic, DNA interstrand crosslinking agent, 5-(aziridin-1-yl)-4-hydroxylamino-2-nitrobenzamide, is formed from 5-(aziridin-1-yl)-2,4-dinitrobenzamide (CB 1954) by a nitroreductase enzyme in walker carcinoma cells. *Biochemical Pharmacology*, *37*(24), 4661–4669. https://doi.org/10.1016/0006-2952(88)90335-8

Komori, T. (2010). Regulation of bone development and extracellular matrix protein genes by RUNX2. *Cell and Tissue Research*. https://doi.org/10.1007/s00441-009-0832-8

Laforest, L., Brown, C. W., Poleo, G., Géraudie, J., Tada, M., Ekker, M., & Akimenko, M. a. (1998). Involvement of the sonic hedgehog, patched 1 and bmp2 genes in patterning of the zebrafish dermal fin rays. *Development (Cambridge, England)*, *125*(21), 4175–4184.

Lalonde, Robert L. Akimenko, M. (2017). Effects of fin fold mesenchyme ablation on zebrafish fin development. *PLoS ONE*.

Laue, K., Pogoda, H. M., Daniel, P. B., Van Haeringen, A., Alanay, Y., Von Ameln, S., … Robertson, S. P. (2011). Craniosynostosis and multiple skeletal anomalies in humans and zebrafish result from a defect in the localized degradation of retinoic acid. *American Journal of Human Genetics*, *89*(5), 595–606. https://doi.org/10.1016/j.ajhg.2011.09.015

Lee, Y. (2005). Fgf signaling instructs position-dependent growth rate during zebrafish fin regeneration. *Development*, *132*(23), 5173–5183. https://doi.org/10.1242/dev.02101

Lee, Y., Grill, S., Sanchez, A., Murphy-Ryan, M., & Poss, K. D. (2005). Fgf signaling instructs position-dependent growth rate during zebrafish fin regeneration. *Development (Cambridge, England)*, *132*(23), 5173–83. https://doi.org/10.1242/dev.02101

Li, N., Felber, K., Elks, P., Croucher, P., & Roehl, H. H. (2009). Tracking gene expression during zebrafish osteoblast differentiation. *Developmental Dynamics : An Official Publication of the American Association of Anatomists*, *238*(2), 459–66. https://doi.org/10.1002/dvdy.21838

Li, X., Montgomery, J., Cheng, W., Noh, J. H., Hyde, D. R., & Li, L. (2012). Pineal photoreceptor cells are required for maintaining the circadian rhythms of behavioral visual sensitivity in zebrafish. *PLoS ONE*, *7*(7). https://doi.org/10.1371/journal.pone.0040508

Mackie, E. J., Ahmed, Y. A., Tatarczuch, L., Chen, K. S., & Mirams, M. (2008). Endochondral ossification: How cartilage is converted into bone in the developing skeleton. *International Journal of Biochemistry and Cell Biology*. https://doi.org/10.1016/j.biocel.2007.06.009

Mackie, E. J., Tatarczuch, L., & Mirams, M. (2011). The skeleton: A multi-functional complex

organ. The growth plate chondrocyte and endochondral ossification. *Journal of Endocrinology*. https://doi.org/10.1530/JOE-11-0048

Maden, M. (1992). A history of regeneration research. Milestones in the evolution of a science. *Cell*, *69*(5), 723–724. https://doi.org/10.1016/0092-8674(92)90282-H

Mao, B., Wu, W., Li, Y., Hoppe, D., Stannek, P., Glinka, a, & Niehrs, C. (2001). LDL-receptor-related protein 6 is a receptor for Dickkopf proteins. *Nature*, *411*(6835), 321–325. https://doi.org/10.1038/35077108

Molven, a, Wright, C. V, Bremiller, R., De Robertis, E. M., & Kimmel, C. B. (1990). Expression of a homeobox gene product in normal and mutant zebrafish embryos: evolution of the tetrapod body plan. *Development (Cambridge, England)*, *109*(2), 279–88. Retrieved from http://www.ncbi.nlm.nih.gov/pubmed/1976086

Moss, J. B., Koustubhan, P., Greenman, M., Parsons, M. J., Walter, I., & Moss, L. G. (2009). Regeneration of the pancreas in adult zebrafish. *Diabetes*, *58*(8), 1844–1851. https://doi.org/10.2337/db08-0628

Münch, J., González-Rajal, A., & de la Pompa, J. L. (2013). Notch regulates blastema proliferation and prevents differentiation during adult zebrafish fin regeneration. *Development (Cambridge, England)*, *140*(7), 1402–11. https://doi.org/10.1242/dev.087346

Nakamura, T., Gehrke, A. R., Lemberg, J., Szymaszek, J., & Shubin, N. H. (2016). Digits and fin rays share common developmental histories. *Nature*, *537*(7619), 225–228. https://doi.org/10.1038/nature19322

Ohgo, S., Itoh, A., Suzuki, M., Satoh, A., Yokoyama, H., & Tamura, K. (2010). Analysis of hoxa11

and hoxa13 expression during patternless limb regeneration in Xenopus. *Developmental Biology*, *338*(2), 148–157. https://doi.org/10.1016/j.ydbio.2009.11.026

Oliver, G., Sidell, N., Fiske, W., Heinzmann, C., Mohandas, T., Sparkes, R. S., & De Robertis, E. M. (1989). Complementary homeo protein gradients in developing limb buds. *Genes & Development*, *3*(5), 641–650. https://doi.org/10.1101/gad.3.5.641

Pacifici, M., Koyama, E., Shibukawa, Y., Wu, C., Tamamura, Y., Enomoto-Iwamoto, M., & Iwamoto, M. (2006). Cellular and molecular mechanisms of synovial joint and articular cartilage formation. In *Annals of the New York Academy of Sciences* (Vol. 1068, pp. 74–86). https://doi.org/10.1196/annals.1346.010

Petrie, T. A., Strand, N. S., Yang, C.-T., Rabinowitz, J. S., & Moon, R. T. (2015). Macrophages modulate adult zebrafish tail fin regeneration. *Development*, *142*(2), 406–406. https://doi.org/10.1242/dev.120642

Pfefferli, C., & Jaźwińska, A. (2015). The art of fin regeneration in zebrafish. *Regeneration*. https://doi.org/10.1002/reg2.33

Pierre Marie Auguste Broussonet. (1789). Memoir on the regeneration of certain parts of the bodies of fishes. *Proprietors and Sold*.

Pisharath, H., Rhee, J. M., Swanson, M. A., Leach, S. D., & Parsons, M. J. (2007). Targeted ablation of beta cells in the embryonic zebrafish pancreas using E. coli nitroreductase. *Mechanisms of Development*, *124*(3), 218–229. https://doi.org/10.1016/j.mod.2006.11.005

Poss, K. D., Shen, J., Nechiporuk, A., McMahon, G., Thisse, B., Thisse, C., & Keating, M. T. (2000). Roles for Fgf signaling during zebrafish fin regeneration. *Developmental Biology*,

222(2), 347–358. https://doi.org/10.1006/dbio.2000.9722

Poss, K. D., Shen, J., Nechiporuk, a, McMahon, G., Thisse, B., Thisse, C., & Keating, M. T. (2000). Roles for Fgf signaling during zebrafish fin regeneration. *Developmental Biology*, *222*, 347–358. https://doi.org/10.1006/dbio.2000.9722

Quarto, N., & Longaker, M. T. (2006). The zebrafish (Danio rerio): A model system for cranial suture patterning. *Cells Tissues Organs*, *181*(2), 109–118. https://doi.org/10.1159/000091100

Quint, E., Smith, A., Avaron, F., Laforest, L., Miles, J., Gaffield, W., & Akimenko, M. A. (2002). Bone patterning is altered in the regenerating zebrafish caudal fin after ectopic expression of sonic hedgehog and bmp2b or exposure to cyclopamine. *Proc Natl Acad Sci U S A*, *99*(13), 8713–8718. https://doi.org/10.1073/pnas.122571799

Rhee, D. K., Marcelino, J., Baker, M., Gong, Y., Smits, P., Lefebvre, V., … Carpten, J. D. (2005). The secreted glycoprotein lubricin protects cartilage surfaces and inhibits synovial cell overgrowth. *Journal of Clinical Investigation*, *115*(3), 622–631. https://doi.org/10.1172/JCI200522263

Rolland-Lagan, a.-G., Paquette, M., Tweedle, V., & Akimenko, M. -a. (2012). Morphogen-based simulation model of ray growth and joint patterning during fin development and regeneration. *Development*, *139*(6), 1188–1197. https://doi.org/10.1242/dev.073452

Ryan, M. D., King, A. M. Q., & Thomas, G. P. (1991). Cleavage of foot-and-mouth disease virus polyprotein is mediated by residues located within a 19 amino acid sequence. *Journal of General Virology*, *72*(11), 2727–2732. https://doi.org/10.1099/0022-1317-72-11-2727

Satoh, A., Mitogawa, K., & Makanae, A. (2015). Regeneration inducers in limb regeneration.

Development Growth and Differentiation. https://doi.org/10.1111/dgd.12230

Schier, A. F., & Talbot, W. S. (2005). Molecular genetics of axis formation in zebrafish. *Annual Review of Genetics*, *39*, 561–613. https://doi.org/10.1146/annurev.genet.37.110801.143752

Schulte, C. J., Allen, C., England, S. J., Juárez-Morales, J. L., & Lewis, K. E. (2011). Evx1 is required for joint formation in zebrafish fin dermoskeleton. *Developmental Dynamics*, *240*(5), 1240–1248. https://doi.org/10.1002/dvdy.22534

Shin, D., Weidinger, G., Moon, R. T., & Stainier, D. Y. R. (2012). Intrinsic and extrinsic modifiers of the regulative capacity of the developing liver. *Mechanisms of Development*, *128*(11–12), 525–535. https://doi.org/10.1016/j.mod.2012.01.005

Simões, M. G., Bensimon-Brito, A., Fonseca, M., Farinho, A., Valério, F., Sousa, S., … Jacinto, A. (2014). Denervation impairs regeneration of amputated zebrafish fins. *BMC Developmental Biology*, *14*(1), 49. https://doi.org/10.1186/s12861-014-0049-2

Sims, K., Eble, D. M., & Iovine, M. K. (2009). Connexin43 regulates joint location in zebrafish fins. *Developmental Biology*, *327*(2), 410–418. https://doi.org/10.1016/j.ydbio.2008.12.027

Singh, S. P., Holdway, J. E., & Poss, K. D. (2012). Regeneration of Amputated Zebrafish Fin Rays from De Novo Osteoblasts. *Developmental Cell*, *22*(4), 879–886. https://doi.org/10.1016/j.devcel.2012.03.006

Slack, J. M. W., Lin, G., & Chen, Y. (2008). Molecular and cellular basis of regeneration and tissue repair: The Xenopus tadpole: A new model for regeneration research. *Cellular and Molecular Life Sciences*. https://doi.org/10.1007/s00018-007-7431-1

Smith, A., Avaron, F., Guay, D., Padhi, B. K., & Akimenko, M. A. (2006). Inhibition of BMP

signaling during zebrafish fin regeneration disrupts fin growth and scleroblast differentiation and function. *Developmental Biology*, *299*(2), 438–454. https://doi.org/10.1016/j.ydbio.2006.08.016

Sternberg, N. (1981). Bacteriophage P1 site-specific recombination. *Journal of Molecular Biology*, *150*(4), 603–608. https://doi.org/10.1016/0022-2836(81)90384-3

Stewart, S., Gomez, A. W., Armstrong, B. E., Henner, A., & Stankunas, K. (2014). Sequential and opposing activities of Wnt and BMP coordinate zebrafish bone regeneration. *Cell Reports*, *6*(3), 482–498. https://doi.org/10.1016/j.celrep.2014.01.010

Summersgill, J. T., Schupp, L. G., & Raff, M. J. (1982). Comparative penetration of metronidazole, clindamycin, chloramphenicol, cefoxitin, ticarcillin, and moxalactam into bone. *Antimicrobial Agents and Chemotherapy*, *21*(4), 601–603. https://doi.org/10.1128/AAC.21.4.601.Updated

Thummel, R., Burket, C. T., Brewer, J. L., Sarras, M. P., Li, L., Perry, M., … Godwin, A. R. (2005). Cre-mediated site-specific recombination in zebrafish embryos. *Developmental Dynamics*, *233*(4), 1366–1377. https://doi.org/10.1002/dvdy.20475

Ton, Q. V., & Iovine, M. K. (2013). Identification of an evx1-dependent joint-formation pathway during FIN regeneration. *PLoS ONE*, *8*(11). https://doi.org/10.1371/journal.pone.0081240

Trujillo, M. E., Pajvani, U. B., & Scherer, P. E. (2005). Apoptosis through targeted activation of caspase8 (“ATTAC-mice”): Novel mouse models of inducible and reversible tissue ablation. *Cell Cycle*. https://doi.org/10.4161/cc.4.9.2030

Tu, S., & Johnson, S. L. (2011). Fate restriction in the growing and regenerating zebrafish fin.

Developmental Cell, *20*(5), 725–732. https://doi.org/10.1016/j.devcel.2011.04.013

van Eeden, F. J., Granato, M., Schach, U., Brand, M., Furutani-Seiki, M., Haffter, P., … Nüsslein-Volhard, C. (1996). Genetic analysis of fin formation in the zebrafish, Danio rerio. *Development (Cambridge, England)*, *123*(Table 1), 255–262.

Weber, T., Namikawa, K., Winter, B., Müller-Brown, K., Kühn, R., Wurst, W., & Köster, R. W. (2016). Caspase-mediated apoptosis induction in zebrafish cerebellar Purkinje neurons. *Development*, *143*(22), 4279–4287. https://doi.org/10.1242/dev.122721

Wehner, D., Cizelsky, W., Vasudevaro, M., Özhan, G., Haase, C., Kagermeier-Schenk, B., … Weidinger, G. (2014). Wnt/??-catenin signaling defines organizing centers that orchestrate growth and differentiation of the regenerating zebrafish caudal fin. *Cell Reports*, *6*(3), 467–481. https://doi.org/10.1016/j.celrep.2013.12.036

Weiss, P. (1947). The problem of specificity in growth and development. *The Yale Journal of Biology and Medicine*, *19*(3), 235.

Westerfield, M. (2007). The Zebrafish Book. A Guide for the Laboratory Use of Zebrafish (Danio rerio), 5th Edition. *University of Oregon Press, Eugene (Book)*.

White, D. T., & Mumm, J. S. (2013). The nitroreductase system of inducible targeted ablation facilitates cell-specific regenerative studies in zebrafish. *Methods*, *62*(3), 232–240. https://doi.org/10.1016/j.ymeth.2013.03.017

Yoshinari, N., Ishida, T., Kudo, A., & Kawakami, A. (2009). Gene expression and functional analysis of zebrafish larval fin fold regeneration. *Developmental Biology*, *325*(1), 71–81. https://doi.org/10.1016/j.ydbio.2008.09.028

Zenno, S., Koike, H., Tanokura, M., & Saigo, K. (1996). Gene cloning, purification, and characterization of NfsB, a minor oxygen-insensitive nitroreductase from Escherichia coli, similar in biochemical properties to FRase I, the major flavin reductase in Vibrio fischeri. *Journal of Biochemistry*, *120*(4), 736–44. https://doi.org/10.1093/oxfordjournals.jbchem.a021473